Journal of Chromatography A, 1218 (2011) 4078–4103

Contents lists available at ScienceDirect

Journal of Chromatography A

journal homepage: www.elsevier.com/locate/chroma

Review

Flow field-flow fractionation for the analysis and characterization of natural colloids and manufactured nanoparticles in environmental systems: A critical review

M. Baalousha*, B. Stolpe, J.R. Lead

School of Geography, Earth and Environmental Sciences, University of Birmingham, Edgbaston B15 2TT, UK

ARTICLE INFO

Article history:
Available online 6 May 2011

Keywords:
Field flow fractionation
Natural and manufactured nanoparticles
Natural colloids
Detection system

ABSTRACT

The use of flow field flow fractionation (FlFFF) for the separation and characterization of natural colloids and nanoparticles has increased in the last few decades. More recently, it has become a popular method for the characterization of manufactured nanoparticles. Unlike conventional filtration methods, FlFFF provides a continuous and high-resolution separation of nanoparticles as a function of their diffusion coefficient, hence the interest for use in determining particle size distribution. Moreover, when coupled to other detectors such as inductively coupled plasma-mass spectroscopy, light scattering, UV-absorbance, fluorescence, transmission electron microscopy, and atomic force microscopy, FlFFF provides a wealth of information on particle properties including, size, shape, structural parameters, chemical composition and particle-contaminant association. This paper will critically review the application of FlFFF for the characterization of natural colloids and natural and manufactured nanoparticles. Emphasis will be given to the detection systems that can be used to characterize the nanoparticles eluted from the FlFFF system, the obtained information and advantages and limitation of FlFFF compared to other fractionation and particle sizing techniques. This review will help users understand (i) the theoretical principles and experimental consideration of the FlFFF, (ii) the range of analytical tools that can be used to further characterize the nanoparticles after fractionation by FlFFF, (iii) how FlFFF results are compared to other analytical techniques and (iv) the range of applications of FlFFF for natural and manufactured NPs.

Contents

* Corresponding author. Tel.: +44 01214147297.
E-mail addresses: m.a.baalousha@bham.ac.uk, mbalousha@yahoo.co.uk (M. Baalousha).

0021-9673/$ – see front matter © 2011 Elsevier B.V. All rights reserved.
doi:10.1016/j.chroma.2011.04.063

1. Introduction

Understanding the properties, fate, behaviour and effects of natural colloids and natural and manufactured nanoparticles (NPs) in the environment is crucially dependent on accurate measurement of their size distribution. In the natural environment, NP size and related properties determine their interaction with contaminants [1], aggregation [2] and fate and transport [3,4]. In (eco)toxicological studies, size is an important factor determining NP toxicity [5], by controlling the biological uptake [6], transport across the blood–brain barrier [7] and the production of reactive oxygen species [8]. Additionally, size is the main parameter used so far to define natural colloids and natural and manufactured NPs. Here, we define manufactured NPs as purposefully produced material with at least one dimension in the size range 1–100 nm within the framework of nanotechnology [9–11]. Natural colloids will be defined as organic or inorganic entities, naturally occurring in the environment with at least one dimension in the size range of 1–1000 nm, according to the International Union of Pure and Applied Chemistry (IUPAC) definition [12]. Natural NPs are subcategory of natural colloids and can be defined as organic or inorganic entities naturally occurring in the environment within the size range 1–100 nm [13,14]. Natural and manufactured NPs exhibit aggregation phenomena in environmentally relevant systems and therefore this review will report some studies where the measured sizes exceed the upper limit of the definition of NPs (i.e. 100 nm) [15–17].

Field-flow fractionation (FFF) is a family of chromatography-like separation techniques used for particle and macromolecule sizing and separation [18]. In recent years, the use of FFF has dramatically increased in a wide range of research areas, including pharmaceutical [19], biomedical [20] and environmental science [21]. Applications of FFF include the separation and characterization of proteins [22], polymers [23], polysaccharides and supramolecular assemblies [24], cells [25,26], natural NPs [21] and more recently manufactured NPs [27,28]. The FFF theory was first proposed by Giddings in the 1960s [29] and since then different sub-techniques of FFF has been developed including flow (FlFFF), sedimentation (SdFFF), thermal (ThFFF), electrical (ElFFF) and gravitational (GrFFF) [18]. When applied to the same samples, these sub-techniques provide complementary information [30]. This review focuses on FlFFF as it is currently the most widely used and versatile technique for natural colloids and natural and manufactured NPs [27,31]. The increased use of FlFFF can be related to (i) its applicability range (1 nm to 50 μm, depending on the applied mode), which covers the full size range of natural colloids (i.e. 1–1000 nm) and natural and manufactured NPs (1–100 nm) [31], (ii) its compatibility to carrier solutions with a wide range of pH and ionic strengths, making it possible to match carrier solution and sample composition [32], (iii) the possibility of rapid on-channel concentration to avoid the perturbations of the sample which can occur during off-line preconcentration [33] and (iv) the possibility of both on-line hyphenation to a wide range of detectors, and collection of sample fractions for further off-line analysis [34]. Detectors that can be combined with FlFFF include on-line detectors such as UV–VIS [35], organic carbon detector [35], fluorescence [36], inductively coupled plasma-mass spectroscopy [37], laser-induced breakdown detection [38], laser light scattering [39], dynamic light scattering [40]; and off-line techniques such as atomic force microscopy [41,42] and transmission electron microscopy [43,44]. The principles, advantages and limitations of the different detectors, and the data they can provide, will be discussed in this paper. In particular, we will concentrate on applications of FlFFF for the characterization of natural colloids and natural and manufactured NPs in natural waters, wastewater, soil, sediments, groundwater, atmosphere and biological samples. Operational considerations, advantages and limitations as compared to other separation techniques will be critically discussed, and recommendations of how to best use the technique will be given.

2. Theoretical background

2.1. FlFFF theory

The theory of FlFFF was developed mainly by Giddings and coworkers [29] and is described in detail elsewhere [35,45]. Briefly, FlFFF is a chromatography-like elution technique based on hydrodynamic principles, in which particles are separated due to their interaction with a cross flow of carrier liquid, applied over the cross section of a thin, flat channel. The walls of the channel are permeable (in case of symmetrical FlFFF, see Section 2.3 for more details about asymmetrical FlFFF), allowing the cross flow to pass through the channel, but the wall through which the cross flow exit the channel (the accumulation wall) is covered by an ultrafiltration membrane, retaining particles in the channel. The sample is eluted along the channel by a longitudinal channel flow, perpendicular to the cross flow. Although the particles are in constant Brownian motion in all directions, the cross flow will shift their average cross-sectional position closer to the accumulation wall. Due to the opposed movements of field transport and Brownian motion, a population of particles with the same diffusion coefficient will form an "equilibrium cloud", whose thickness, l, depends on the cross-flow

induced velocity, U, and the diffusion coefficient of the particles, D (Eq. (1)):

$$l = \frac{D}{U} \quad (1)$$

In a polydisperse sample, populations of particles with different diffusion coefficients will thus have different values of l.

Due to the geometry of the channel, the longitudinal channel flow will be laminar, with a parabolic flow profile. Since the velocity of the parabolic flow vectors decreases toward the walls of the channel, the transport velocity of particles along the channel will increase with l. Thus, particle retention is a function of diffusion coefficient, and particles with different diffusion coefficients will be separated. In FlFFF, particle retention volume can be related to diffusion coefficient and volumetric cross flow velocity, V_c, as shown in Eq. (2):

$$D = \frac{\lambda V_c w^2}{V^0} \quad (2)$$

where V^0 is the void volume and λ is the retention parameter, which is the ratio of the cloud thickness to the channel thickness l/w. λ can be calculated from the measured retention volume V_r using the general FlFFF retention equation (Eq. (3))

$$R = \frac{V^0}{V_r} = 6\lambda\left(\coth\frac{1}{2\lambda} - 2\lambda\right) \quad (3)$$

where R is referred to as the retention ratio. For nanoparticles which are strongly retained ($V_r > 6V^0$), Eq. (3) can be approximated to (Eq. (4)):

$$\frac{V^0}{V_r} = 6\lambda \quad (4)$$

Hydrodynamic diameter (d_h), e.g. the diameter of a compact sphere with the same diffusion coefficient as the particle, can be calculated from diffusion coefficient, applying the Stokes–Einstein equation (Eq. (5)):

$$d_h = \frac{kT}{3\pi\eta D} \quad (5)$$

where k is the Boltzmann constant, T is the temperature and η is the viscosity of the carrier liquid.

2.2. Fractionation modes of FlFFF

Two fractionation modes are possible in an FlFFF system: normal and steric/hyperlayer. The normal (Brownian) mode presented above prevails when nano-sized and slightly larger particles (1 nm to ~0.5 μm) are separated, and results in smaller particles eluting before larger particles. The steric/hyperlayer mode can occur due to lift forces (or "slip" forces) when very larger particles come in close proximity to the accumulation wall, and permits larger particles elute faster than smaller particles [46–48]. This mode occurs in the fractionation of micron sized particles. The particle size at which steric inversion occurs depends on several factors such as channel thickness, flow rate, field strength, and particle shape [47,49]. For instance, the steric inversion point shifts to larger sizes with the decrease of the cross flow [49]. Combining both possible elution modes gives FlFFF the theoretical ability to fractionate particles from 1 nm to ~100 μm of diameter. However, analysis of samples spanning a broad size range may hamper the separation process and results in co-elution of small particles (eluting in normal mode) and very large particles (eluting sterically). Such behaviour can only be monitored by applying an independent size characterization technique such as laser light scattering, transmission electron microscopy and atomic force microscopy [41,43].

2.3. Types of available FlFFF

Two types of FlFFF are today in use: symmetrical (FlFFF) and asymmetrical (AsFlFFF). AsFlFFF is witnessing an increased popularity and has been used in most of the more recent publications. In both symmetrical FlFFF and AsFlFFF, the channel is made out of two Perspex blocks separated by a spacer, which defines the channel geometry and thickness. In symmetrical FlFFF, permeable ceramic frits mounted in the Perspex blocks compose the walls of the channel. The accumulation wall is covered by an ultrafiltration membrane, typically with a cut-off of 1–10 kDa (Fig. 1a). Both the channel flow and the cross-flow can be delivered by HPLC-pumps. Alternatively, in many applications the cross-flow has been maintained in a closed circuit by a double piston syringe pump. The fractionation process starts with the injection of the sample (typically 10–100 μL) through the channel inlet by the use of an injection loop and valve. After a few seconds, when the sample has reached a few cm into the channel, the channel flow is stopped and only cross flow is allowed to pass through the channel. During this 'relaxation' step, equilibrium is reached between cross-flow driven transport and Brownian motion of the particles, according to Eq. (1). The time of the relaxation step is typically chosen to allow three channel volumes of cross flow pass the channel. Thereafter, the channel flow is again turned on, and the sample is eluted along the channel and separated according to Eq. (3). The advantages of a closed-circuit cross-flow delivery by the double-piston pump are that makes it much easier to maintain stable flow rates through the channel, and that less carrier liquid is used. However, the disadvantage is recirculation of substances which pass the membrane into the channel via the top frit, which may deteriorate the baseline of the detectors and cause errors in chemical measurements.

In AsFlFFF, only the accumulation wall is composed of a permeable ceramic frit, while the upper wall is impermeable (Fig. 1b). Carrier flow enters the channel through the inlet at the tip of the channel (V_{in}), and exits the channel both through the accumulation wall membrane (V_c) and through the channel outlet (V_{out}). Thus, the inlet flow generates both the cross-flow and the longitudinal flow in the channel, and $V_{in} = V_{out} + V_c$. To compensate for the reduction in the volumetric flow along the channel, keeping the velocity of the longitudinal flow constant, the AsFlFFF channel has the shape of a trapezoid, decreasing in width from the channel inlet to the outlet (Fig. 1b). The injection is performed by direct injection into the inlet carrier stream or via an additional port slightly downstream of the channel inlet (Fig. 1b) through a step called (focus step). This provides the advantage of sample focusing and the injection of large sample volumes without decreasing the fractionation performance (on-channel pre-concentration). During the focus step, the carrier flow is directed from the inlet and outlet into the channel with flow rates $V_{in} \ll V_{out}$. By adjusting the two opposed flow rates, it is possible to define a certain zone in the channel where the lateral flow is virtually zero and the flow vectors in the channel are pointing at this zone (Fig. 1b). If the sample is injected into this zone it will be focused and it is possible to perform a line-start for the following fractionation independent of the sample volume injected. Fig. 1b shows the procedures of an AsFlFFF run, with the focusing/injection step and the elution step.

3. Experimental considerations

3.1. Calibration methods

FlFFF theory (normal mode only, see Section 2.1) allows the calculation of the diffusion coefficient and equivalent hydrodynamic diameter of particles, directly from their retention time and the channel dimensions. However, the accumulation wall membrane used in FlFFF will protrude into the channel, and therefore

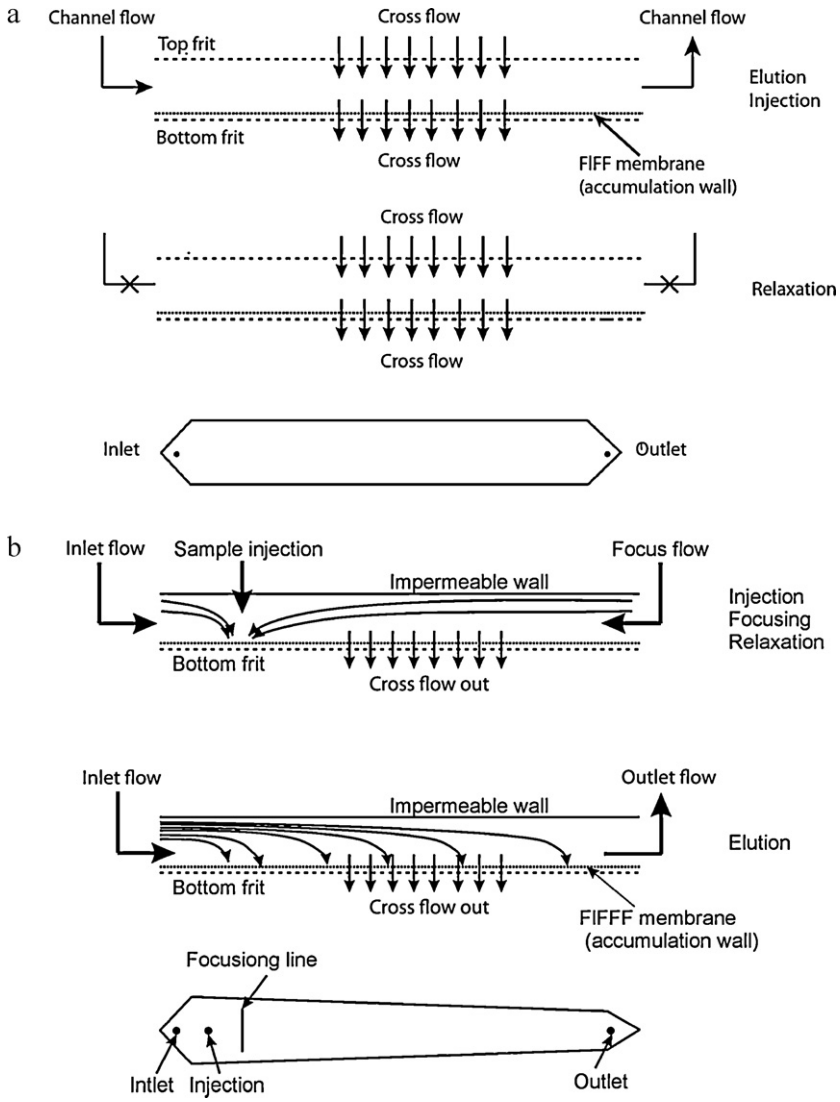

Fig. 1. Schematic representation of the available FlFFF systems, (a) symmetric FlFFF Flow scheme and channel geometry and (b) typical asymmetrical FlFFF channel.

influence w (and V^0), which therefore must be determined experimentally each time the membrane is changed or the carrier solution is altered. In earlier works, V^0 was usually determined by measuring "void time" or "breakthrough time" of very small or very large macromolecules/particles with the cross flow turned off [50,51]. However, since the accumulation wall membrane is flexible, w can be expected to depend on both cross flow and carrier liquid composition. Therefore, a preferred method is the calibration of w by spherical standards of tabulated diffusion coefficients/known size, using the same flow rates and carrier composition as the sample, without changing the carrier after the analysis of the sample [52].

Alternatively, without any determination of channel dimensions, a series of standard NPs covering the range of NP sizes being separated can be used to plot a calibration curve between D or d_h and V_r (normal mode, Eqs. (2)–(4)) [39,43]. This relationship can then be used to determine the size of unknown particles. This calibration method should also allow the determination of D or d_h when gradient cross flow is used, or when particles are separated under steric mode (see Section 2.2), where the mathematical expression for FlFFF theory are extremely complex and are not yet available.

Several studies have used FlFFF to determine the molar mass (MM) of natural organic macromolecules (i.e. natural NPs). This parameter is of interest since environmental samples have traditionally been fractionated using ultrafiltration, in which the cut-offs of filtration membranes are defined by MM instead of size. The method requires the calibration of the relationship between V_r and MM, using a calibration standard with a similar structure and behaviour as the macromolecules in the sample. Beckett et al. showed that a set of polystyrene sulfonates (PSS) with different MM could be used as calibration standards for natural humic substances [53]. Plotting the logarithm of MM for the PSS standards to the logarithms of D determined by FlFFF theory yielded a straight calibration line. Several workers have confirmed the appropriateness of PSS standard for calibrating the retention time to the MM in the analysis of humic acids by FlFFF [53] or size exclusion chromatography (SEC) under specific conditions [54]. A potential source of error in most of these studies arises from the use of UV detection, which has a higher sensitivity for aromatic and other UV-adsorbing moieties in the molecule.

The representation and accuracy of the obtained diffusion coefficient, size distribution or molar mass is always limited by how well the calibration standards represent the studied particles. So far, the use of latex beads has been reported for calibration of the size distribution of natural and manufactured NPs. Whereas latex beads are hard spheres, this is rarely the case for natural and manufac-

tured NPs [41,44]. Natural NPs are usually coated by natural organic macromolecules and manufactured NPs are usually coated by various types of capping agents. In the use of PSS as *MM*-standards for humic substances, Dycus et al. [55] reported that a single relationship correlating the substances to PSS could not be identified, since PSS and humic substances may not have the same dependency of *D* on *MM* under varying solution conditions (pH and ionic strength). Similar variations in *D* with different solution conditions can be expected for humic substances from different sources, causing undetermined amounts of systematic error in the values of *MM* reported below.

3.2. Sample preparation

FlFFF is a dynamic technique that provides reasonable size fractionation of suspensions of particles in the size range of 1–500 nm over a wide range of pH and ionic strengths. However, as natural colloids and natural and manufactured NPs are most likely to be part of complex matrices, sample preparation may be necessary including: (i) NP extraction, (ii) NP separation from larger particles and (iii) sample concentration (see Tables 2 and 4).

The first step in sample preparation is the extraction of NPs from their matrices (e.g. natural water, soil, sediment or biological tissues). Different methods have been used for the extraction of natural NPs from their matrices and manufactured NPs from biological media (see Tables 2 and 4), which depends on the sample matrix composition. For instance, compost leachates have been prepared by simple dilution in pure water [56]; sediment samples have been prepared by a homoionic exchange and peptization with NaCl solution followed by washing with deionised water [57]; soil samples have been prepared by washing with acetic acid to dissolve the carbonate cement and break soil aggregates to obtain the constituent NPs [39]; NPs from biological tissue have been extracted by enzymatic digestion [58] or acid digestion [59]. The second step involves NP separation from larger particles or aggregates. This can be achieved by sedimentation [39,44], centrifugation [57] or filtration [56]. The advantages and limitations of these methods are described in more detail elsewhere [60]. The third step is sample concentration. Small sample (injection) volumes and large dilution on-channel make pre-concentration necessary before the characterization of many environmental samples, due to their low concentrations of NPs. Many different pre-concentration methods have been used, including ultrafiltration, coagulation and centrifugation [61]. These methods may result in particle destabilization and aggregation, altering the particle size distribution. To overcome artifacts, such as aggregation of NPs, which occur during harsh and lengthy pre-concentration, Wahlund and Giddings developed an on-channel concentration method for AsFlFFF [62], which was later modified for use in FlFFF [33,63] and has been successfully used in several studies [64–70]. A large volume of sample (up to 100 mL) can be injected into the channel (usually through the channel outlet), and by choosing a high value of the outlet/inlet flow ratio (typically 12), the NPs in the sample will be concentrated in a focus point a few cm from the channel inlet. The focusing step is followed by the relaxation step, and the FlFFF run is processed as normal.

The on-channel concentration method has now been integrated as the standard method for injection of samples in modern AsFlFFF instruments. In addition to allowing the injection of larger samples, the focusing method has the advantage of focusing the sample in a narrow zone at the start of the fractionation, thereby minimizing band broadening. Moreover, by using the same cross flow during the focusing step as during the elution step, equilibrium between cross-flow driven transport and Brownian motion of the particles can be reached without the need for an additional relaxation.

3.3. Method optimisation

FlFFF provides a high resolution separation of NPs. However, FlFFF separation can be compromised through several processes such as (i) particle aggregation, (ii) particle membrane interaction, (iii) pre-elution due to sample overloading or inter-particle electrostatic repulsion, and (iv) steric inversion [56,60,71]. Such processes should be monitored and minimized in the method optimisation step. Method optimisation is an essential step in FlFFF experimentation in order to achieve a good separation and reduce sample perturbation. Method optimisation should account for (i) the choice of the carrier solution, (ii) the choice of the accumulation wall membrane and (iii) the choice of the applied field (cross flow).

Ideally the carrier solution should mimic the physicochemical properties of the NP suspension (e.g. pH, ionic strength and chemical composition) to minimize NP perturbation such as surface charge, double layer thickness, particle aggregation/disaggregation and dissolution. However, usually a simple solution of electrolyte at ionic strength and pH condition close to the real sample is selected (see Tables 2 and 4). Additionally, in some cases a surfactant is used to maximize sample recovery, and a bactericide (e.g. sodium aside) is used to prevent bacterial growth [43], although changes from the in situ conditions are more likely. In all cases the carrier solution should be selected to prevent particle aggregation, particle–membrane interaction, particle dissolution and bacterial growth, as well as to maximize particle recovery.

The accumulation wall membrane should be selected to retain all NPs in the channel, to minimize particle–membrane interaction and to maximize NP recovery. The most widely used membranes in FlFFF are regenerated cellulose and polyethersulfonate with a molecular cut-off in the range of 300–10,000 Da (see Tables 2 and 4). To minimize NP losses, in particular those in the size range of 1 nm such as humic substances, the smallest membrane cut-off should be used. To minimize particle–membrane interaction and maximize sample recovery, a charged membrane (same charge as the particles) should be used [56].

The cross flow is the key factor that determine FlFFF resolution and quality of separation. The cross flow should be optimised to achieve the best possible separation while keeping sample losses and void-peak–sample-peak overlap to minimum [39]. Additionally the cross flow should be selected according to the size of the NPs under consideration. For instance, a high cross flow should be applied for the fractionation of small NPs whereas a low cross flow should be applied for the fractionation of large NPs (see Tables 2 and 4). For a heterogeneous sample with a wide size distribution, a gradient flow should be applied to reduce sample analysis time and minimize steric inversion effect [56]. Alternatively, a range of cross flows should be applied for heterogeneous samples, in parallel to using an independent size detector technique to assess any fractionation abnormalities [39].

The quality of separation can be evaluated by sample recovery, fractogram reproducibility, absence or minimal height of the void peak, absence or minimal overlap between the void peak and the fractionated NP peak, absence of steric inversion and through the use of independent particle sizing detector such as multi angle laser light scattering, dynamic light scattering, transmission electron microscope and atomic force microscope (see Section 4 for more details).

4. Detectors: multi method approach

As described above, FlFFF theory (see Section 2.1) can be applied for the determination of NP diffusion coefficient, and thus, the equivalent hydrodynamic diameter, if the channel dimensions and

the run conditions are known (see Section 3.1) and no abnormal effects, such as particle membrane interaction, are present. Calculation of the hydrodynamic diameter is based on applying Stokes' relationship assuming that particles are hard spheres. This is not always the case, suggesting the need for a detector giving an independent and complimentary measurement of the particle size distribution. In addition, this approach can be used to verify any abnormalities and/or deviation from theoretical principles of the fractionation [41,43]. Moreover, on-line or off-line detectors can provide a wide range of information on other particle properties such as composition, concentration [72], optical properties [73–75], interaction with trace metals [64–66,76,77] and structure [41,44,78]. This section gives an overview of the different techniques that have been used in the literature as detectors after the FlFFF system including on-line coupling, i.e. the direct transient analysis of the FlFFF effluent, and off-line coupling, i.e. the collection of fractions of the FlFFF effluent for later analysis. It also provides a discussion of the extra information and advantages that can be achieved from the on-line/off-line coupling.

4.1. UV–VIS

In most of the studies cited here, UV–VIS has been used as an on-line turbidity detector with FlFFF, and it has often been assumed that UV absorbance is proportional to particle concentration. However, UV-absorbance is a complex parameter, depending on both light absorption and diffraction, and varies with the wavelength of the light, the size of the particles, and the composition of the chromophores in natural organic matter. The light absorption of aromatic and phenolic organic functional groups is much stronger than of other organic and inorganic NPs [79]. Moreover, the molar absorptivity of humic substances at 280 nm has been shown to increase with MM [80], and the wavelength of maximum absorbance has been found to increase with MM of the humic substances [81,82]. As a result, several studies have found the UV-absorbance size distribution to be biased toward larger sizes relative to the mass distribution [81,82]. The bias was not large enough to prevent meaningful comparisons between results achieved at short wavelengths (220–280 nm), but it became significant at longer wavelengths (280–380 nm), resulting in large variations in the apparent MM (7–63%). Therefore, Zhou et al. recommended that 254 nm should be used as the wavelength, except for at low carbon concentrations where 230 nm was recommended due to better sensitivity [82]. For manufactured NPs, the UV wavelength should be chosen according to their maximum absorbance. For instance, UV 400 and 254 nm were used to detect silver NPs and organic surface coating [83].

4.2. Organic carbon detector

A large fraction of natural NPs in environmental samples are composed of organic material. The higher sensitivity of UV–VIS for aromatic organic compounds compared with other type of organic matter has created a need for a detector that can quantify dissolved organic carbon (DOC) coupled on-line to FlFFF. Reszat and Hendry modified a total organic carbon (TOC)-analyser to allow a continuous analysis of organic carbon at the low flow rate normally used in FlFFF [84]. In the TOC-analyser, inorganic carbon is removed, and the organic carbon is oxidized with ammonium persulfate and UV irradiation. The CO_2 subsequently produced is quantified with a conductivity sensor. With a channel flow rate of 1.5 mL min^{-1}, fractograms could be recorded with one data point every 4 s, allowing the determination of the continuous DOC size distribution in the 0–10 kDa range. Results showed that the DOC-distribution for both isolated humic substances and natural groundwater had a shape similar to the UV–VIS-distribution, but was shifted to smaller sizes by about 0.2 kDa [84].

4.3. Fluorescence

Fluorescence is the light emission as a result of the return of electrons from a singlet excited state to a singlet ground state. The sample is irradiated with light of a certain "excitation wavelength" (λ_{ex}), and the intensity of the emitted light is measured at a certain "emission wavelength" (λ_{em}), at 90° angle relative to the pathway of λ_{ex}. The combination of two wavelengths makes fluorescence detection highly specific for certain organic substances. Coupled on-line to FlFFF, fluorescence has been used to determine the continuous size distribution of humic substances [66,85,86] and protein-like substances [36,65,73] in environmental samples. It has also been used to distinguish humic substances adsorbed to inorganic colloids from "free" humic macromolecules [87]. In addition, a fluorescence detector can be used as a nephelometric turbidity detector by setting the excitation wavelength equal to the emission wavelength ($\lambda_{ex} = \lambda_{em}$), thereby measuring light scattered by particles at 90° angle from the incident light beam. For more details on this mode, the reader is referred to the article by Kammer et al. [88].

4.4. ICP-MS and ICP-OES

One of the most important functions of natural NPs in aquatic systems is their capacity to bind and transport large amounts of trace elements. The combination of the continuous fractionation of FlFFF with sensitive techniques for multi-elemental analysis has the potential to increase our knowledge about size-dependent variations in composition and trace-element interactions of natural NPs. Inductively coupled plasma-optical emission spectrometry (ICP-OES), graphite furnace atomic absorption spectrometry (GFAAS) and inductively couples plasma-mass spectrometry (ICP-MS) have been coupled on-line and off-line to FlFFF. For a deeper insight in the method, we refer to a recent review [37]. In both ICP-OES and ICP-MS, the liquid sample is nebulised to an aerosol, and the components in the sample are atomised and ionised in a plasma at about 6000–10,000 K, produced by electromagnetic induction in ionised argon gas [89]. While ICP-OES detects the different elements by their specific light emission induced by the excitation of atom ions in the plasma, ICP-MS use a mass spectrometer to separate and quantify the ions of different elements. The coupling of FlFFF to ICP-MS was first proposed by Beckett [90], the first applications with off-line coupling to SdFFF were performed by Chittleborough et al. [91] and Taylor et al. [92], while Murphy [93] was the first to couple ICP-MS on-line to SdFFF. During the 1990s, ICP-MS was almost exclusively used as a detector for SdFFF, but during the last 10 years on-line coupling to FlFFF, first described by Hassellöv et al. has become increasingly popular [76]. The first studies described the colloidal size distribution of Mg, Al, Si, Fe and Rb, but with the improvement in sensitivity, resolution and scanning frequency of ICP-MS instruments the number of element that can be analysed have increased. By the on-line coupling of high resolution sector field ICP-MS to FlFFF, the colloidal size distributions and concentrations of 45 elements could be determined in one single measurement [67].

4.5. Laser-induced breakdown detection (LIBD)

Laser-induced breakdown detection (LIBD) is a highly sensitive method for the detection of NPs and colloids in the size range of 10–400 nm [94,95], down to the nanogram per litre range. During the detection process, plasma is generated on single particles by a focused laser beam and the resulting light emissions are detected

optically. The method is based on the difference in breakdown thresholds of liquid and solid matter, which is lower for solid material. The laser pulse energy is adjusted precisely so that in the pure liquid no breakdown events occur, and only in the presence of colloids, the breakdown threshold in the focal volume is exceeded. The spatial distribution of several thousand recorded plasma flashes within the focal volume reveals the mean particle diameter. The evaluation of the number of breakdown events per number of laser pulses results in a breakdown probability, together with the particle size, the concentration is calculated using specially designed computer software. Compared to conventional laser light scattering methods, the LIBD is approximately 6 orders of magnitude more sensitive for particles smaller than ca. 50 nm [94,95]. LIBD signal has smaller dependency on particle size compared to light scattering techniques and photon correlation spectroscopy, hence the higher sensitivity of the LIBD for small colloids compared to PCS and LLS [96]. The total number of particles down to 10 nm and the average particle diameter can be determined accurately with LIBD method [97]. Kwegi and co-workers showed that LIBD becomes more sensitive for smaller particles after removal of larger particles, suggesting that FlFFF can improve the performance of LIBD. Bouby et al. demonstrated the sensitivity of the FlFFF-LIBD hyphenation, showing a detection limit of 1, 4 and 20 μg/L for a mixture of 20, 50 and 100 nm polystyrene reference particles respectively, which corresponds to an injected mass of 1, 4 and 20 pg. This detection limit was lower for iron oxide particles and it was of the order of 240 μg/L [38].

4.6. Multi angle light scattering (MALS)

MALS is a characterization technique that collects the light scattered by particles in a suspension at different angles and uses it to determine the absolute molar mass and size of particles (radius of gyration, R_g). The radius of gyration is the root mean square distance of the particle's parts from its centre of gravity i.e. it represents the distribution of mass within the particle.

Hyphenation of FlFFF and MALS provide a good solution to overcome the limitations presented by their separate use for the analysis of complex and heterogeneous samples of natural and manufactured NPs in environmental systems. In theory, FlFFF can be used on its own for particle size measurement, but the complexity of natural and manufactured NPs may result in abnormalities in the separation process that cannot be detected unless an independent measurement of particle size is performed, which can be performed by MALS. On the other hand, the polydispersity of natural and manufactured NPs may hamper size measurement by MALS. Here, FlFFF can play a vital role by providing a sample separation before MALS analysis [39,98]. Furthermore, hyphenation of FlFFF-MALS can offer a further insight into particle characterization by providing information on particle shape in parallel to particle size by calculating a shape factor $\rho = R_g/R_h$. This shape factor has a value of 0.775 for spherical particles and increases as particles deviate from the spherical shape [39,98–100].

4.7. Dynamic light scattering (DLS)

DLS is a technique that measures the diffusion coefficient of particles moving under Brownian diffusion conditions. It does so by correlation of the fluctuations of the scattered light intensity over time to extract the diffusion coefficient. The particle size can then be calculated applying Stokes–Einstein equation.

DLS can be used as an on-line detector for FlFFF and provides comparable information on particle hydrodynamic diameter [40]. Such hyphenation provides a solution for the limitations presented by each method separately. FlFFF provides a less polydisperse fraction that can improve DLS analysis and DLS can be used as quality assurance for the fractionation behaviour inside the FlFFF channel as DLS is an absolute size measurement technique.

4.8. Transmission electron microscopy (TEM)

TEM is a characterization technique based on a single particle analysis. TEM uses an electron beam to illuminate a sample. The transmitted electrons form an image of the sample that can be magnified and projected into an imaging device, usually a photographic film or a CDD type camera. TEM provides a wealth of information of particle properties including direct visual information about particle size and shape, crystallographic structure and chemical information when coupled to specific detectors (X-ray energy dispersive spectroscopy (X-EDS) and electron energy loss spectroscopy (EELS)). Nonetheless, TEM analysis are tedious and appropriate sampling and sample handling procedures should be followed to obtain environmentally representative information as described elsewhere [17,101].

TEM can be performed on fractions collected after separation by FlFFF, to confirm particle size and to verify the separation performance of the FlFFF [43]. Combined together, FlFFF and TEM can be used to calculate particle thickness [44,102]. Chemical analysis by X-EDS can be performed on fractions collected after FlFFF separation and ICP-MS analysis to confirm the composition of natural NPs and the associated metals [72]. This combination of bulk (ICP-MS) and single particle (TEM) analysis can be a particularly powerful method.

4.9. Atomic force microscopy (AFM)

AFM is a microscopy technique which maps a surface topography using a flexible force-sensing cantilever–tip system. The interaction force between the cantilever–tip and the sample surface causes minute deflections of the cantilever, which are detected by an optical system composed of a laser and a photodetector [103]. The surface of the sample beneath the tip is typically scanned using a piezoelectric tube coupled to a feedback system that moves the sample (z stage) up-and-down to keep the cantilever deflection and the sample–tip interaction force constant giving a topography image [103]. These images can be used to measure particle height, or diameter assuming spherical shape of the particles.

As with the TEM, AFM can be performed on fractions collected after separation by FlFFF, to confirm particle size and to verify the separation performance of the FlFFF [42]. Comparing the particle sizes measured by FlFFF and AFM can provide quantitative information on particle shape and/or permeability [41]. AFM can also help to identify the types of natural NPs separated by FlFFF in complex environmental samples, based on their morphology variations [66].

4.10. Comparison between detectors

Comparison of the signals obtained by the different detectors is not straightforward and need to be considered carefully. Their signals are weighted differently e.g. number, weight, mass and intensity (see Table 1) giving rise to different size averages e.g. number, weight, mass and z-average, respectively. These distribution and averages are correlated differently to the particle size (e.g. number $\sim d$, weight $\sim d^3$, mass $\sim d^3$ and intensity $\sim d^6$). Fig. 2 shows an example of natural colloidal sample analysed by FlFFF-UV, FLD and ICP-MS-MALS. Both the UV signal and the Al signal detected by ICP-MS coincide, while the FLD (in scattering mode) and MALS signals are shifted toward larger sizes [72]. Both UV and ICP-MS detection give a mass weighted distribution, which is the same as the volume weight distribution for a constant particle density through the size distribution, and therefore, these distributions

Table 1
Comparison between the techniques that can be used as on-line or off-line detectors with FlFFF.

Method	Measured parameter	Distribution weighting	Relation to diameter	Calculated average	Information provided on coupling	Order of detection limit	References
UV	Chromophores	Weight	$\sim d^3$	Weight	Relative concentration	μg/L to mg/L	[65]
FLD	Fluorophores	Weight	$\sim d^3$	Weight	Relative concentration	μg/L	[63]
OCD	CO_2	Mass	$\sim d^3$	Mass	Carbon concentration	mg/L	[73]
ICP-MS	Metal concentration	Mass	$\sim d^3$	Mass	Elemental composition Trace metal concentration	μg/L range ng/L potentially	[65,72]
LIBD	Particle number and size	Number	$\sim d$	Number	Number particle concentration	ng/L range	[96]
MALLS	Radius of gyration	Intensity	$\sim d^6$	Z	Shape factor	μg/L to mg/L	[72]
TEM	Projected area	Number	$\sim d$	Number	Particle shape	mg/L	[44]
AFM	Height above surface	Number	$\sim d$	Number	Permeability and sphericity	mg/L	[41]

UV: ultraviolet; FLD: fluorescence detector; OCD: organic carbon detector; ICP-MS: inductively coupled plasma-mass spectroscopy; LIBD: laser-induced breakdown detection; MALLS: multi angle laser light scattering; TEM: transmission electronic microscopy; AFM: atomic force microscopy.

may coincide [72]. However, FLD in scattering mode and MALS give intensity weighted size distributions and hence the shift toward larger sizes. Fig. 3 shows an example of a natural NP sample analysed by FlFFF-UV jointly with AFM and TEM. Fig. 3 shows that the UV signal is shifted toward larger particles compared to AFM and TEM; however, conversion from UV volume weighted PSD to number PSD shows a better agreement between the three signals [41]. Therefore, in order to compare FlFFF size distribution obtained different detectors, it is essential to understand the principles of the detectors used and the type of the size distribution they provide. Conversions of mass or volume to number particle size distribution is described in [41] and from intensity to number size distribution is described in [104].

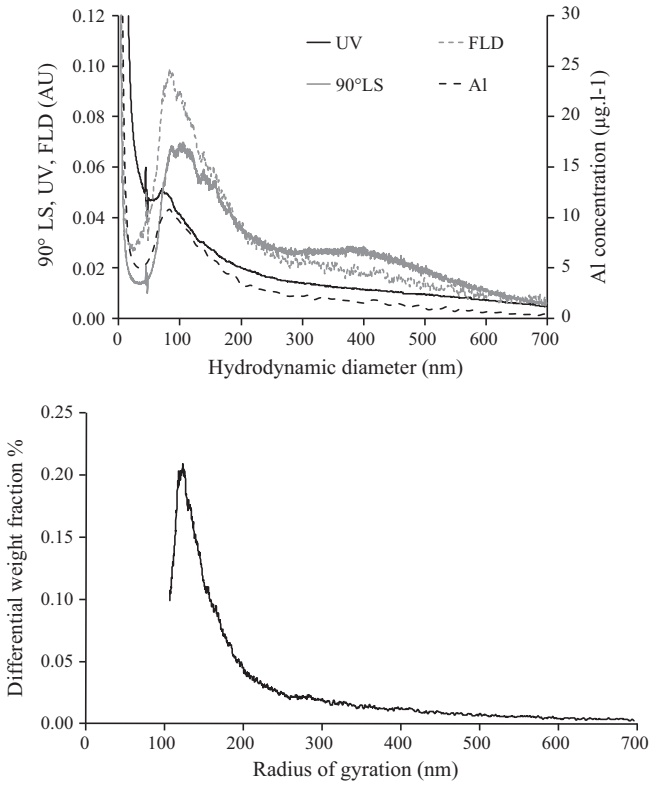

Fig. 2. Characterization of natural river colloids by FlFFF-multi detection system (a) comparison between MALS-UV-FLD-ICP-MS signals showing a good agreement between UV and ICP-MS signals and a slight shift toward larger particles for the FLD and MALS signals and (b) radius of gyration calculated from MALS showing a shift toward larger sizes compared to the hydrodynamic diameter obtained by FlFFF. Figure modified from Baalousha et al. [72].

For natural colloids and natural NPs, rarely spherical, comparison between sizing techniques has been used to obtain information on particle shape and structure. For instance, the ratio of the hydrodynamic diameter measured by FlFFF and the radius of gyration measured by MALS was used as an indication of particle shape [39,44]. The ratio of the hydrodynamic diameter measured by FlFFF and the particle height measured by AFM was used as an indication of particle permeability and shape [41].

5. Comparison to other fractionation methods

When compared to other particle fractionation techniques such as filtration, ultrafiltration, cross-flow ultrafiltration and centrifugation, FlFFF has the advantage of providing continuous particle size separation, high resolution and minimal perturbation, although preconcentration and on-channel concentration may lead to artifacts. In addition, the poorly studied area of contaminant-particle on-channel re-equilibration may be a particular problem in environmental studies; in metal analysis, only the operationally defined non-labile fraction in a particular size range is measured, while cross contamination may be likely due to complex dissociation. The extent of this effect is unknown and requires further investigation. Ultrafiltration (UF) and size exclusion chromatography (SEC) are two methods that have been widely applied for the separation and fractionation of natural NPs. UF is a discrete fractionation technique, whereas SEC is a continuous size fractionation technique, like FlFFF. However, FlFFF has a better size resolution than UF and SEC methods. For instance, Bolea et al. have used UF, SEC and AsFlFFF for the characterization of a compost leachate, showing a fairly consistent size classification for organic matter and most of the metal ions, even though slight disagreements were observed [105]. All three methods showed that the main fraction of compost leachate organic matter is smaller than 10 kDa. The deviation in *MM* obtained by ultrafiltration compared to SEC and FlFFF and between the *MM* measured by SEC and FlFFF was attributed to the differences in the separation principles, sample recoveries and the different reference materials used for calibration. Ultrafiltration was calibrated with a globular protein, whereas SEC and FlFFF were calibrated with polyethersulfonate (PSS) standards [105]. Assemi et al. applied FlFFF for the characterization of NOM fractions obtained by UF (<0.5, 0.5–3, 3–10, 10–30 and >30 kDa) and suggested that the separation by UF does not produce the expected MM and size [50]. The size and *MM* obtained by FlFFF of the large UF fractions were smaller than the UF nominal filter range. On the other hand, the lower size fractions contained molecules with higher *MM* than the nominal UF membrane cut-off, suggesting the passage of large molecules through the filters. This has been related to the possibility of passage of lose aggre-

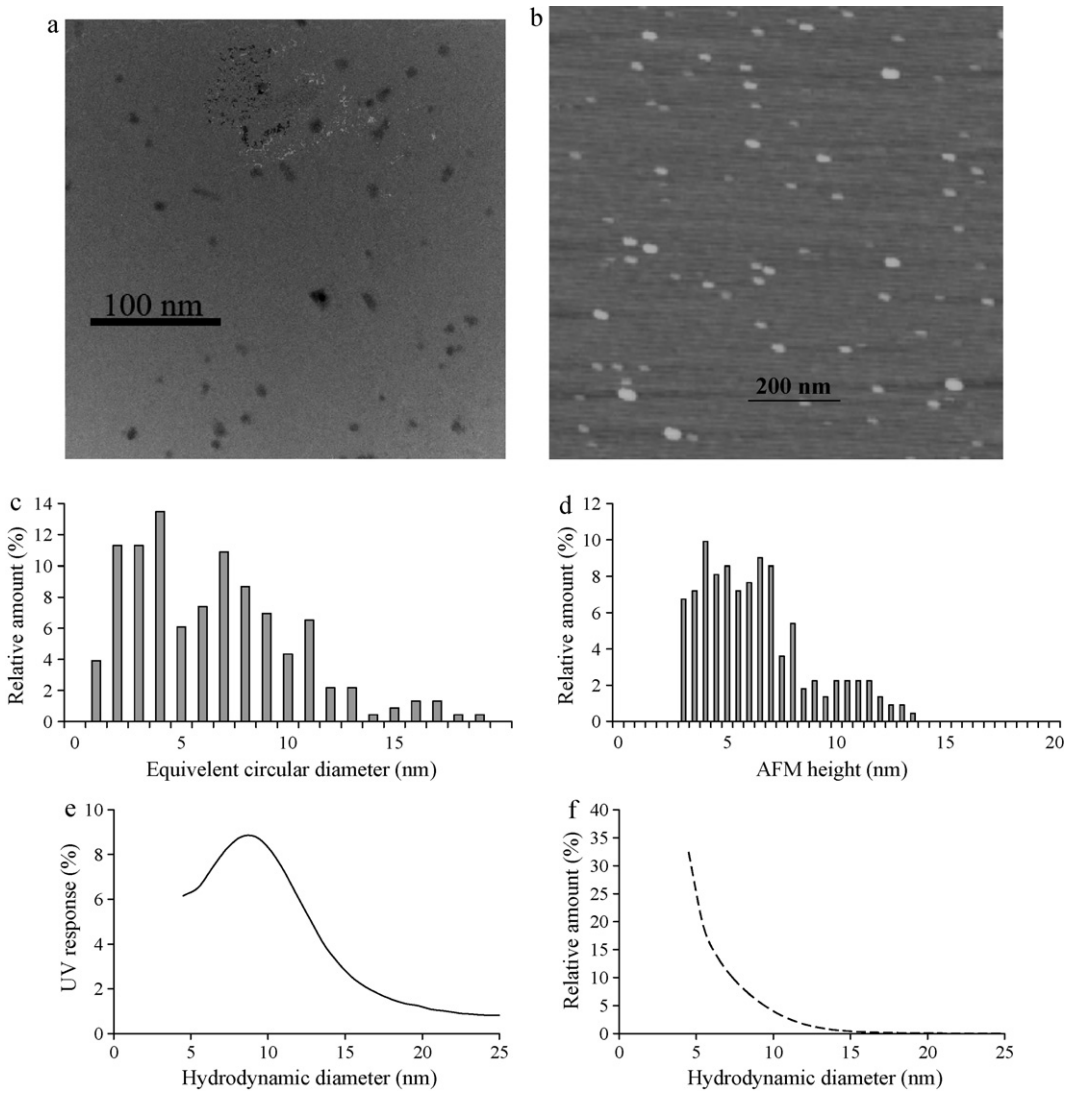

Fig. 3. Iron oxide NPs (200 mg/L Fe) reference solution characterization: (a) transmission electron microscopy (TEM) micrograph; (b) atomic force microscopy (AFM) micrograph; (c) equivalent circular diameter histogram calculated from TEM micrograph; (d) particles height histogram measured by AFM; (e) hydrodynamic diameter for iron oxide NPs at pH 2 in the absence of humic acid measured by flow-field flow fractionation-UV and (f) same fractogram as (e) with conversion into number particle size distribution. Figure modified from Baalousha et al. [15].

gates through the filters even when the aggregate size is larger than the pore size. They suggested that the separation was determined not only by size, but also by the molecular structure of the NOM. The results indicate that great caution needs to be exercised when interpreting molecular size and speciation results for humic substances obtained by UF [50]. Additionally, ultrafiltration membranes were found to retain large amounts of organic matter with sizes considerably smaller than the membrane cut-off [50,106]. The pore size in the filtration and ultrafiltration methods are not exact and may contain a certain fraction of smaller or larger pores. Additionally, membrane cut-offs are not the unique parameter determining retention of natural organic matter compounds. However, size exclusion, electrostatic repulsion, and NOM aromaticity all influenced the retention of NOM [107]. Therefore, FlFFF is considered more accurate for the determination of organic matter *MM* than filtration and ultrafiltration techniques. Nevertheless, ultrafiltration have certain advantages over FlFFF including provision of nearly 100% recovery (when operated under the right conditions) and retaining the particles in the original medium, i.e. they are not exposed to a carrier solution as they are in FlFFF. Therefore, ultrafiltration-providing near-complete recovery and fractionation of NPs under realistic conditions, and FlFFF -providing the continuous size distribution of NPs, should be a powerful combination in studies of complex samples such as natural water.

An important issue to be considered when comparing the *MM* measured by UF and FlFFF is the standards used to calibrate each method. In UF, the *MM* cut-offs (MWCO) of the individual filter membranes are calibrated by globular proteins, whereas in FlFFF, the *MM* is usually calibrated with polystyrene sulfonate (PSS) standards. Therefore, *MM* information may deviate from one method to another [105].

Comparison of the FlFFF with SEC, both coupled to MALS, for the fractionation of coil shaped dissolved dextrans showed higher polydispersity (M_w/M_n) by FlFFF (2.5 times) compared to SEC, suggesting better separation by FlFFF compared to SEC, owe to FlFFF higher separation resolution. The high molar mass molecules were better separated by FlFFF. This is because the upper working limit of FlFFF is much higher than SEC, where exclusion effect takes place depending on the column pore size [108].

6. Comparison to other sizing techniques

There is a wide range of analytical tools that can used to measure the size of natural and manufactured NPs. The most commonly used summarized is Table 6, together with the measured and calculated parameters and the type of the average size calculated from each method. The theoretical principles of these techniques are beyond the scope of this paper and are described elsewhere (see references below and in Table 6). The differences in theoretical principles, measured parameters and the type of average size may result in large variation of the measured size/size distribution, particularly for polydisperse samples. This complicates any attempt to directly compare the measured sizes, and usually the comparison is used to verify the observed trends in particle size rather than verifying the exact values [43,44]. Direct comparison of the values of the measured sizes is only possible for monodisperse hard spheres (see Fig. 3), where all the measured parameters will converge to a similar value, given that the proper conversion of size distribution is performed [15]. For instance, conversion of the volume size distribution of natural NPs obtained by FlFFF-UV to number size distribution and comparison to the size distribution measured by AFM [41] and conversion of all sizes measured by FlFFF, AUC, DLS, XRD and TEM of ZnS NPs [109] showed a good agreement between the measured sizes with only little differences. Plaschke et al. measured the particle size distribution of disk-like shaped bentonite colloids by different methods including FlFFF, LIBD, AFM and photocorrelation spectroscopy (PCS) [96]. A fair agreement was found between sizes measured by AFM (73 nm, number weighted), FlFFF (~235 nm mass weighted and ~70 nm number weighted peak maximum) and LIBD (67 ± 13 nm, number weighted). However, larger sizes (235 nm intensity-weighted, 138 nm when converted to number-weighted) were obtained by PCS. They suggested the need to apply a correction factor for particle shape and a conversion of distribution weighting in order to compare particle size distribution [96]. Another comparative study of characterization of NPs (TiO_2 and quantum dots) by FlFFF compared to other techniques including TEM, atomic force microscopy (AFM), nanoparticle tracking analysis (NTA), fluorescence correlation spectroscopy (FCS) and DLS was performed by Domingos et al. [17]. Again, measured sizes showed some significant discrepancies, mainly due to particle aggregation and differences between the measured size parameters. All these studies suggest that there is no best technique for size determination of NP size, but a combination of several techniques including FlFFF is the best approach to determine NP size [17,96,109].

Therefore, understanding the principles of particle sizing methods, the measured parameters, the weighted averages (see Table 6) and conversions of all results to one weighted average (mass, volume or number) are essential for intercomparison between the measurement obtained by the different techniques.

7. Advantages and limitations of FlFFF

FlFFF is a versatile and flexible separation technique based on hydrodynamic principles. It has a major advantage of separating particles continuously, non-destructively, at high resolution within the size 1 nm to 100 μm. However, individual separations can only be performed in smaller windows, of about an order of magnitude for any individual run, according to the applied separation mode (normal or hyperlayer) and the separation conditions i.e. cross flow and channel flow (see Tables 2 and 4). FlFFF has been used for separating particles as small as 1 nm such as humic substances [110]; particles in the range 20–450 nm such as natural colloidal particles [43] and particles in the range 5–100 μm such as clay minerals [46–48]. Another major advantage of the FlFFF is the possibility to couple either on-line or off-line to a wide range of detectors such as UV, FLD, DOC, ICP-MS, LIBD, MALS, TEM and AFM (see Section 4). This flexibility provides a wide range of particle properties including size distribution, chemical composition, particle-associated contaminants, particle number concentration and particle structure (see Tables 3 and 5 and Sections 5 and 6).

Unlike liquid chromatography techniques, the particle separation takes place in an open channel, where no stationary phase is required. This important feature makes FlFFF potentially a minimally perturbing technique. For instance, molecular degradation, particle adsorption to stationary phase and size exclusion are minimized [111,112].

Although FlFFF has several advantages compared to other separation and fractionation techniques, there are limitations to the method such as material losses, particle–membrane interaction, sample dilution, washing of sample components and overloading. Material losses due to sample–membrane interaction and adsorption can be significant and may represent up to 50% of the injected mass [27]. The two major causes of material losses in FlFFF are the permeation NPs through the accumulation wall membrane, and adsorption of NPs onto the surface of the membrane [113,114]. Permeation of NPs through the membrane is mainly a problem with small NPs (close to the cut-off of the membrane), and depends on the pore sizes of the membrane and on charge repulsion and double layer repulsion between the membrane and the NPs. The adsorption of NPs to the membrane surface is a result of attractive forces, such as van der Waals, hydrophobic and charge interactions, and can be expected to be more severe for large NPs. For FlFFF, most studies of natural and manufactured NPs have used accumulation wall membranes of either regenerated cellulose (RC) or polyethersulfone (PES). A few studies have also used membranes of cellulose acetate (CA). PES membranes are relatively hydrophobic (based on water droplet contact angle) and have a high negative surface charge (based on zeta potential), while RC membranes are more hydrophilic and have a lower negative surface [107,115,116]. In comparison, PES membranes have been found to be more effective than RC membranes in retaining small (a few nm) organic matter in natural water, due to higher charge repulsion between the membrane and organic macromolecules [107,115,116]. On the other hand, adsorptive losses due to hydrophobic interactions between organic matter and the membrane were more severe with the PES membrane. Both permeation through, and adsorption to, the membranes have been found to increase with decreasing pH and increasing Ca^{2+}-concentration, due neutralization of the surface charge and diminishing of the electrical double layer of both organic macromolecules and the membranes [107,115,116]. These findings agree with several studies using FlFFF. For example, Lyven et al. found recoveries of creek water organic matter to be superior with a 1 kDa PES membrane compared with a 1 kDa RC membrane [33]. On the contrary, Thang et al. found a better recovery of isolated humic acid with a 5 kDa RC membrane than with a 2 kDa PES membrane, and determined the losses to be due to adsorption of humic substances to the PES membrane [113]. The differences can be explained by compositional differences of the samples. The creek water organic matter in the first study is likely to be dominated by smaller and relatively hydrophilic fulvic acid, which can easily permeate through the RC membrane, while the more hydrophobic humic acid used in the second study is more likely to adsorb to the PES membrane. Several studies have found that the recoveries of both humic substances and larger soil NPs decrease with decreasing pH and increasing ionic strength of the carrier solution [113,114], in agreement with the decrease in surface charge and double layer thickness of the NPs and the membrane. The use of a carrier with low concentration (1–5 mM) of a monovalent salt and a high pH (>8) has therefore been recommended in studies of NPs in natural samples [71,113]. A surfactant can also be added to the FlFFF carrier in order to decrease the hydrophobic interactions between the NPs

Table 2
Summary of FlFFF operational conditions and analysed natural colloids and natural nanoparticles of selected natural environmental studies.

Water type or location	Device, detectors, membrane	Pretreatment	Carrier solution	Operating conditions	Study objective	Chemical species	References
Humic and fulvic acid in groundwater, clay pore water (Germany), isolated from natural water (UK). Commercial humic acid (Aldrich)	FlFFF (F-1000) UV_{254} 1, 5 and 10 kDa RC (Schleicher and Schuell and Wyatt Technology)	Groundwater samples kept under anaerobic conditions Humic substances isolated on anion exchange column	0.01% Tween + 0.02% NaN_3 0.1 mM NaOH + 0–50 mM $NaClO_4$, pH 10 5 mM Tris, pH 9.1 (optimal) 50 mM Tris, pH 9.1	CF: 1.0 mL min^{-1} XF: 1/3/4/5 mL min^{-1}	Develop method for optimal recovery for humic substances. Testing different membranes and carriers with different compositions and concentrations.	–	[113]
Commercial humic acid (Aldrich)	FlFFF (F-1000) UV_{254}, ICP-MS 1 kDa RC (Postnova)	–	30 mM Tris, pH 7.5	CF 1.0 Ml min^{-1} XF 2.0 mL min^{-1}	Interaction between metal ions and humic substances.	Cd, Cu and Pb	[119]
Loire River and its tributaries, France	FlFFF (F-1000) UV_{254}, $FLD_{250/430}$, LS 90°, MALLS, ICP-MS, STEM-X-EDS 1 kDa RC	0.45 μm and 0.01 μm filtration Preconcentration (25-fold) 1 kDa ultrafiltration	0.025% SDS + 0.02% NaN_3	CF: 1.0 mL min^{-1} XF: 0.25 → 0.1 mL min^{-1} (50 min)	Size based speciation of river NPs and trace metals association to different colloidal phases.	Al, Fe, Mn, Cu, Ni and Pb	[72]
Vail Lake, Bailey Brook River and Tern River, UK	FlFFF (F-1000) UV_{254}, AFM 1 kDa RC	0.025 μm filatration	1 mM $NaNO_3$	CF 1.0 mL min^{-1} XF 3.0 mL min^{-1}	Determination of colloidal particles sphericity and permeability by testing the hard sphere assumption of Stokes–Einstein equation.	–	[41]
Peat-draining rivers in northern Scotland	AsFlFFF (AF-2000) UV_{220}, ICP-MS 1 kDa RC (Postnova)	0.2 μm. Samples stored 1 week before analysis	25 mM NaCl	NR	Determine size of nanoparticulate iron in river water, and its behaviour during mixing with seawater.	Fe	[131]
Rio Negro and small tributaries, Brazil. Podsol water	AsFlFFF (AF-2000) UV_{254}, LS 7-angle 1 kDa RC (Postnova) 10 kDa RC (Postnova)	0.7 μm filtration. Some samples concentrated by reverse osmosis. Samples stored one year before analysis	10 mM $NaNO_3$, pH 5.7	FF: 4/5 mL min^{-1} CF: 1.0 mL min^{-1} XF: 3.09/0.2 5 mL min^{-1}	Determine size distribution of UV-absorbing organic matter, variations with season and between small and large rivers and soil water. Comparison between AsFlFFF and SEC.	–	[126]
River water and coastal seawater, Mississippi and Pearl Rivers and Mississippi Bight, USA	FlFFF (F-1000) UV_{254}, $FLD_{350/480}$, $FLD_{275/340}$, ICP-MS 1 kDa PES (Pall Filtron)	0.45 μm filtration and concentration with 1 kDa ultrafiltration (50-fold)	10 mM NH_4Cl, pH 8 55 mM NH_4Cl, pH 8	FF: 4.5 mL min^{-1} CF: 0.5 mL min^{-1} XF: 3.0 mL min^{-1}	Determine size distributions of coloured organic matter and iron nanoparticles in river and seawater, and their binding of elements. Comparison between rivers with different water chemistries.	P, Mn, Fe, Cu, Zn, Pb and U	[65]
Coastal seawater, Gullmarn Fjord, Sweden	AsFlFFF (AF-2000) UV_{270}, $FLD_{350/450}$, ICP-MS, AFM 1 kDa PES (Pall Filtron)	0.45 μm filtration	55 mM NH_4Cl, 2 mM $(NH_4)_2CO_3$, pH 8	FF: 2.0 mL min^{-1} CF: 0.5 mL min^{-1} XF: 2.0 mL min^{-1}	Characterize the different types of organic NPs binding trace elements in coastal seawater, their sources, formation and seasonal variations.	Fe, Cu, Ag, La, Er and Pb	[66]

Wastewater treatment plant effluent, Lake Geneva water, Switzerland	AsFlFFF (AF-2000)	0.45 μm filtration and concentration with 1 kDa ultrafiltration (12.6–20-fold)	10 mM $NaNO_3$, pH 5.4	FF: 4.0 mL min^{-1} CF: 1.0 mL min^{-1} XF: 0.1/0.25/0.3/0.4/1/3/1 → 0 mL min^{-1}	Characterization of NPs binding elements in wastewater. Different conditions for determination of small (0–15 kDa) and large (10–10,000 kDa) NPs. Distinction between humic substances and biopolymers, based on fluorescence.	Al, Cr, Mn, Fe, Cu, Zn, Ag, Cd and Pb	[140]
Soil extract	AsFlFFF (Eclipse 2) UV_{280}, MALLS 10 kDa RC (Wyatt Technology)	Sieving (32 μm), dispersion in water 3 months, dialysis-cleaning of decantate, settling-removal of unstable colloids during 2 years	1/3/10 mM NH_4NO_3, pH 8	FF: R CF: 1.0 mL min^{-1} XF: 0.3/0.5/0.8 mL min^{-1}	Method optimisation for soil NPs, with respect to recovery and separation efficiency. Variation of cross flow and carrier composition and concentration.	–	[71]
Soil extract	AsFlFFF (Eclipse 2)	Leaching of soil in pure water during 16 h, centrifugation, 0.45 μm filtration of supernatant, spiking with trace metals	1 mM NH_4NO_3 + 0.1 mM SDS, pH 8	FF: 0.75 mL min^{-1} CF: 1.0 mL min^{-1} XF: 0.5 mL min^{--1}	Development of AsFlFFF-ICP-MS for soil nanoparticles. Comparison between on-line and off-line quantification.	Pb, Sn, Se, Sb, Cd and As	[152]
Compost leachate	AsFlFFF (AF-2000) $UV_{190–520}$, ICP-MS 1 kDa RC (Postnova) 1 kDa PES (Postnova)	Suspension of compost in ultrapure water, agitation, settling-removal of large particles, centrifugation of decantate, 0.45 μm filtration of supernatant	Ultrapure water, pH 8	CF: 0.8 mL min^{-1} XF: 0.1/4/5 mL min^{-1}	Method development for characterization of metal association to micro and nano-particles in compost. Combination of normal and steric elution mode.	Al, Si, Pb, Zn and Cu	[56]
River sediment, Clark Fork River, USA.	AsFlFFF (AF-2000) UV_{220}, $FLD_{350/450}$, MALLS, ICP-MS 10 kDa PES (Pall Filtron)	Air-drying of sediment, disaggregation by mortar and 125 μm sieving, suspension in 0.1 M NaCl. Repeated sonication and centrifugation to remove >100 nm particles	0.5 mM $Na_4P_2O_7$	FF: 0.4 mL min^{-1} CF: 1.4 mL min^{-1} XF: 0.4 mL min^{-1}	Determine binding of elements to nanoparticles in rivers sediment.	Mg, Al, Si, Ti, Cr, Mn, Co, Cu, Zn, Sr, In, Ba, La, Ce, Pr, Pb, Bi and Th	[57]
Exhaust from diesel and gasoline engines	FlFFF (homebuilt) UV_{254} 10 kDa RC (Amicon)	Collection of particles on filter, sonication of filters in ethanol. Mixing with hexane and water with 0.05% Triton X-100. Decantation of hexane and heating of water to remove hexane and ethanol residuals	0.05% Triton X-100 + 0.02% NaN_3, pH 8	CF: 4.63 mL min^{-1} XF: 0.60 mL min^{-1}	Determine the size distribution of particles emitted from engines. Comparison between heavy and light-duty diesel engines and gasoline engines. Study variations in size with engine speed and load.	–	[166]

FlFFF: flow field flow fractionation; AsFlFFF: asymmetrical flow field flow fractionation; RC: regenerated cellulose; CF: channel flow; XF: cross flow; FF: focus flow rate; DL: detection limit; PSS: polystyrene sulfonate; SDS: sodium dodecyl sulfate; LS: light scattering; SEM: scanning electron microscopy; kDa: kilo Dalton; VPSD: volume particle size distribution; NPSD: number particle size distribution; STEM: scanning transmission electron microscopy; X-EDS: X-ray energy dispersive spectroscopy; PES: polyether sulfone; NR: not reported.

Table 3
Summary of FlFFF calibration and data quantification methods and major conclusions of selected natural environmental studies.

Water type or location	Sample volume. Size range	Calibration calculation of R_h or *MM*	Calculation quantification	Main conclusions and comments	References
Groundwater and clay pore water (Germany). Fulvic and humic acid isolated from natural water (UK). Commercial humic acid (Aldrich)	0.02 mL 0.5–10 kDa 0.5–18 nm	R_h from FlFFF-theory, channel thickness from t_0 measurements. MM-calibration with PSS and globular proteins	% recoveries reported, but no description of how they were calculated	Humic substance recovery decrease dramatically with increasing cross flow, increasing ionic strength and decreasing pH. Better recovery (less adsorption) with RC membrane than with PES membrane. Low ionic-strength carrier gave overloading with PSS, but not with humic substances. M_w vs. D plots of PSS and globular proteins had different slopes, due to different shapes/densities.	[113]
Commercial humic acid (Aldrich)	0.02 mL 0.5–20 nm	R_h from FlFFF theory. MM from calibration with PSS: 1.4, 4.4 and 43.3 kDa	Breadth of size distribution = particle size range at half peak maximum. The mean particle diameter = the particle size at which 50% of the total cumulative area is detected, calculated from the cumulative size distribution	Size of humic acid around 3.1 nm. Size distribution of Pb was cantered on a larger size compared with humic acid, Cu and Cd. Aggregation in $CaCl_2$ and in seawater resulted in a bimodal size distributions of humic acid and metals (second peak around 6 nm).	[119]
Loire River and its tributaries, France	2 mL 25–1000 nm	Calibration curve using nanospherical polystyrene polymer standards 50, 73, 102, 150, 220, 343, 494 nm	–	Trace metals were associated with three colloidal phases: natural organic matter, iron oxide and aluminium silicates. An excellent methodology to relate colloidal physical (size, surface area and shape) to their chemical properties (chemical composition, surface chemical composition) and to understand colloids-trace metals associations.	[72]
Vail Lake, Bailey Brook River and Tern River, UK	0.02 mL 0.5–10 nm	R_h from FlFFF theory channel calibration with 20 and 30 nm spherical standards	Conversion of VPSD to NPSD and vice versa Particle height (AFM)/particle hydrodynamic diameter (FlFFF)	The assumption of Stokes–Einstein equation was met for the Vale lake sample but not for the Bailey Brook and Tern River samples, indicating that the first sample contain hard sphere particles while the two other samples contain particles that might not be spherical or permeable.	[41]
Soil extract	No info about volume 10–500 nm	R_g calculated from MALLS data. Validation of size using nanospheres	Recovery reported as ratio between the integrated FlFFF-curve with and without cross flow	Best recovery with a carrier with low ionic strength (1 mM), anionic surfactant (0.3 mM SDS) and pH 8. Non-ionic surfactant not applicable. Recovery decreased with increasing cross flow, XF = 0.5 mL min^{-1} was a good compromise between optimized recovery and separation.	[71]
Soil extract	0.15 mL 60–500 nm	R_g calculated from MALLS data	On-line injection of element standards into ICP-MS. Off-line quantification by fraction collection, concentration by freeze-drying, analysis on ICP-MS	On-line and off-line coupling of AsFlFFF to ICP-MS yielded comparable results, but on-line coupling was more convenient. Two populations of NPs, UV-absorbing organic matter and larger (200–500 nm) particles. Cd associated with both populations while As, Se, Sn and Pb associated mainly with the larger particles.	[152]
Rio Negro and small tributaries, Brazil. Podsol water	1.0/0.1 mL 10–150 nm or 0.5–5 nm	R_g calculated from LS-data. R_h calculated from FlFFF-theory, channel thickness determined by calibration with a protein. MM from calibration with PSS	–	M_w of UV-absorbing organic matter was 0.5–2 kDa, decreasing from podsol to small creeks to the large river. A population of larger (60 nm) NPs was detected by MALLS. Good agreement between AsFlFFF and SEC. Reverse osmosis shifted size distribution to slightly smaller sizes.	[126]

Compost leachate	0.1 mL 0.5–17,000 nm	R_h in steric mode calibrated by 0.1–10 μm polystyrene standards. MM in normal mode calibrated by PSS	Recovery reported as the ratio between the integrated FlFFF-curve with and without cross flow	Normal mode gave continuous distribution of particles up to 100 kDa, with Cu and Pb peak maxima shifted to larger sizes relative to UV. Steric elution showed several populations of particles in the 16–17,000 nm size range, the largest particles were rich in Al and Si.	[56]
Peat-draining rivers in northern Scotland	0.1 mL 0.1–100 kDa	MM determined by calibration with PSS	Not specified	Most iron in the 0.2 μm filtered samples was <10 kDa. A bimodal Fe size distribution was observed, the larger population was almost absent at higher salinity. The size of UV-absorbing organic matter increased with salinity.	[131]
River sediment, Clark Fork River, USA.	0.1 mL 20–400 nm	Rg calculated from MALLS data. MM determined by calibration with PSS.	Injection of element standards into the ICP-MS after every run.	Particles distributed over the 20–500 nm size range. All elements enriched in the < 100 nm size range compared with Al. TEM showed elements bind to iron oxyhydroxide NPs, while clay particles were much larger and did not bind many elements.	[57]
River water and coastal seawater, Mississippi and Pearl Rivers and Mississippi Bight, USA	2.5–20 mL 0.5–40 nm	R_h calibrated by proteins with different sizes. MM calibrated by PSS	Injection of element standards into the ICP-MS after every run.	Three populations: 0.5–4 nm humic-like organic matter, 3–8 nm protein-rich organic matter and 5–40 nm iron-rich NPs. All elements associated with the humic-like organic matter, P associated with protein-rich organic matter and P, Mn and Pb associated with Fe-rich NPs. Different sizes of Fe-rich NPs in the different rivers, could be related to water chemistry.	[65]
Coastal seawater, Gullmarn Fjord, Sweden.	120 mL 0.5–35 nm	R_h calculated from FlFFF-theory, channel thickness calibrated by a protein. MM calibrated by PSS	Injection of element standards into the ICP-MS after every run.	3–4 populations: 0.5–4 nm humic-like terrestrial organic matter binding most elements, 3–8 nm marine organic matter (presumed protein) binding Cu and Ag, and 7–40 nm marine organic matter (presumed polysaccharides) binding Fe and Pb. The two larger populations increased in concentration in the early summer.	[66]
Wastewater treatment plant effluent, Lake Geneva water, Switzerland	1 mL 0–15 kDa 10–10,000 kDa	R_h calibrated by sulfate polystyrene latex. MM calibrated by PSS	No quantification. Relative element-concentrations determined by integration of FlFFF-curves	Humic substances were 1.5–3.5 kDa. Several populations of larger NPs with overlapping size distributions, probably biopolymers. All elements associated with humic substances, while Al, Fe and Pb associated also to larger (400–1200 kDa) NPs.	[140]
Exhaust from diesel and gasoline engines	0.1–0.2 mL 24–400 nm	R_h calculated from FlFFF theory, channel thickness determined with rapid breakthrough measurements	No quantification	Particles were distributed over the 50–350 nm size range, with a maximum at 100 nm. No difference in size between heavy and light-duty diesel engines. Turbo-engines has higher percentage <100 nm particles than engines with naturally aspirated inhalation, and catalytic converter gave rise to a narrowing of the size distribution of the particles from gasoline engines	[165]

R_h: hydrodynamic diameter; MM: molar mass; R_g: radius of gyration.

and the membrane, thereby increasing the recovery. It has been shown that an anionic surfactant (e.g. sodium dodecyl sulfate) is preferable to a non-ionic surfactant (Tween) [71]. However, the risk for perturbations of the sample, e.g. disaggregation of NPs and shift in element complexation equilibria has to be taken into account with the use of surfactants in the FlFFF carrier. In addition to the compositions of the accumulation wall membrane and the FlFFF carrier, the recovery of NPs in FlFFF has been shown to decrease rapidly with increasing cross flow [33,71,113]. In addition to causing incomplete recovery, sample–membrane interactions may also cause material retardation, with consequent overestimation of the particle size determined by FlFFF theory. However, combination with detectors such as MALS, TEM and AFM can be applied to verify sample separation and size agreement with theoretical values [43].

The MWCO of the accumulation wall membrane used in FlFFF is usually defined as the size of a spherical NP (usually a globular protein) which is 90% retained by the membrane. However, from the discussion above, it is clear that the effective MWCO depend on several factors, including membrane pore size, charge and composition, charge and shape of the NPs, pH and ionic strength of the sample and FlFFF carrier [107,115,116]. Therefore, results from studies of small NPs, e.g. humic substances, must be treated with caution, especially when samples with varying pH and ionic strength have been analysed. Reported increases in size of humic substances with increasing ionic strength or decreasing pH could potentially be an effect of the permeation of smaller components through the membrane [117–119]. Some studies on NOM have used membranes cut-off of 10 kDa [105,120], which will certainly result in losses of small particles and the overestimation of particle size. Moreover, losses of material must be considered in studies of samples with high salinity using FlFFF. For example, Zanardi-Lamardo et al. found the recovery of UV-absorbing organic matter (relative to total UV-absorbance) to be much lower in seawater samples (5.7–8.1%) than in freshwater samples (35–65%) [121]. The lower recovery in seawater can to some extent be explained by the generally smaller size of marine UV-absorbing organic matter, resulting in that a larger fraction is smaller than the MWCO of the accumulation wall membrane. However, increased permeation through, and adsorption to, the accumulation wall membrane due to the high salinity of seawater are also likely to have influenced the recovery. A common way to verify material losses is by carrying out a mass balance study. This can simply be done by comparing the area under the UV or ICP-MS signal at the applied cross flow to that without applied cross flow [33]. However, since the sample eluted through the channel without cross flow would include also components smaller than the MWCO of the accumulation wall membrane, this method not applicable when studying samples with large amounts of "truly dissolved" (<1 nm or <1 kDa) components. For example, in natural waters, 40–60% of the organic matter and as much as 90–95% of some trace elements (e.g. Cu and Mn) are often found in the <1 kDa fraction (based on ultrafiltration) [65].

Preconcentration [61] or on-channel concentration [33] are often necessary to use prior to the analysis of low-concentrated environmental samples by FlFFF. However, these pretreatments may result in sample alterations, in particular with regard to trace metals and other components loosely bound to the NPs. Preconcentration is usually performed by volume reduction via ultrafiltration or centrifugation, which increases particle concentration and reduces the distance between the particles, possibly bringing them to contact, potentially inducing aggregation of particles or re-conformation of colloidal matter. The same artifacts can be expected to occur during on-channel concentration, in which the focusing process results in high concentration of NPs (>1000 times in natural sample) at a tiny space at the focusing point [77]. Lyven et al. concluded that if aggregation of small colloids occurs during on-channel concentration, it is fast and repeatable even when comparing runs with different cross flows [77]. In addition, on-channel concentration results in continuous washing of the sample with carrier solution, which has the potential to remove large amounts of trace metals weekly bound to natural NPs. This process may be an important limitation in the use of FlFFF-ICP-MS to study NP–trace element interactions, and has not yet been investigated. A reasonable assumption is that results presented from FlFFF-ICP-MS coupling represent the 'non-labile' bound metals rather than the total metals bound to NPs.

Although the volume of injected sample is not a limiting factor when on-channel concentration is used, there is limitation in the amount of sample that can be injected before repulsion between the NPs becomes significant. This repulsion will increase the thickness of the 'sample cloud', e.g. increase the value of l (Eq. (1)), thereby lowering the retention time of the NPs [117]. The effect, which is referred to as 'overloading' can to some extent be overcome by using an FlFFF carrier with a higher ionic strength, since this will diminish the electrical double layer of the NPs. When unknown types of samples are injected, it is necessary to inject different volumes and check whether the retention times differ significantly [122].

A major disadvantage of FlFFF is the change in chemistry of the medium surrounding the NPs during the fractionation, from the sample to the FlFFF carrier. Changes in ionic strength, pH and concentrations of Ca^{2+} and Mg^{2+} may induce aggregation, disaggregation or conformational changes of the NPs [71,113]. When studying components associated with NPs, such as element NP-interactions using FlFFF-ICP-MS, the 'washing' of the NPs with a carrier made up of ultrapure water can be expected to result in that only components that are strongly bound to the NPs are detected. Attempts to match the composition of the FlFFF carrier to the composition of the sample must be weighed against the needs to minimize sample losses (by the use of a low-ionic strength, high pH carrier with added surfactant) and overloading effects (by the use of a carrier with higher ionic strength). Matching of the FlFFF-carrier to the sample is especially problematic in the analysis of seawater samples, with an ionic strength of up to 0.7 M, and high concentrations of Ca^{2+} and Mg^{2+}. Williams and Keil showed that the use of UV-oxidized seawater as a carrier in FlFFF caused a complete adsorption of PSS-molecules from a sample, due to the collapsing of the electric double layer at such high ionic strength [123]. In field studies of marine samples where seawater has been used as the carrier, the average hydrodynamic diameter of UV-absorbing organic matter has been much larger [74,124], than in studies in which a carrier with a lower ionic strength has been used [65,66,125]. These differences can most likely be explained by lower recoveries of humic substances when seawater was used as the carrier. In the coupling of FlFFF to ICP-MS, seawater cannot be used as the carrier, since even low salt concentrations give rise to a dramatic degradation in the ICP-MS response [68], and high salt concentrations can even damage the ICP-MS.

AsFlFFF technique provides several advantages in comparison to SFlFFF such as: (i) transparent top-wall, which allows checking the flow streams and the focusing performance using coloured polymers (e.g. dextran-blue), (ii) simpler channel handling and membrane replacement, (iii) sample volume does not affect fractionation thanks to the focusing process, (iv) on channel concentration of dilute samples, (v) better fractionation resolution thanks to sample focusing process, (vi) better detection limit thanks to less sample dilution, and (vii) lower risk of contamination from the top frit when it is coupled to elemental analysis such as ICP-MS. Nonetheless, there still some drawbacks such as: (i) abnormal separation behaviour observed to start around 500 nm particle diameter, (ii) fractionation theory is more complex, (iii) possible

contamination with particles from previous runs during focusing process, especially in case of old channel membrane.

8. Applications for natural colloids and nanoparticles

FlFFF has been widely used for the characterization of natural colloids, natural NPs and organic macromolecules. Tables 2 and 3 provide a summary of selected studies together with a general overview of the experimental conditions, sample treatment, calibration and quantification methods and the main findings of these studies. These tables can provide a quick guideline for FlFFF users of the optimum experimental, operational and calculation methods required for the different types and size fractions of NPs. Below is a more detailed discussion of the applications of FlFFF for the characterization of natural colloids and NPs in the different environmental compartments including: (i) river and lake waters, (ii) estuaries and marine water, (iii) wastewater, (iv) soil, sediment and groundwater and (v) atmospheric particles. A separate section is devoted to extracted humic substances due to their relevance to the different environmental compartments. Humic substances are the most common organic NPs found in natural river and lake-waters and in soils [105]. Many studies have therefore used concentrated solutions of isolated and purified humic and fulvic acid to develop FlFFF methods to be used for natural samples, or to model how these important NPs are influenced e.g. by changes in ionic strength or pH. Results from these studies can be used to optimise FlFFF methods including the choice of carrier solution, accumulation wall membranes and flow rates when FlFFF is used to study natural samples. Additionally, there are very limited number of studies using FlFFF for the fractionation of other natural organic matter components such as fibrils due to their heavy interaction with the FlFFF membrane [98].

8.1. Extracted humic substances

Beckett et al. first reported the use of FlFFF-UV to determine the size distribution of fulvic and humic acid extracts [53]. Diffusion coefficients of the different acids were found to be in the range $\sim 3–4 \times 10^{-10}\ m^2\ s^{-1}$ (corresponding to a hydrodynamic diameter of ~1–1.5 nm) and number averaged MM was determined to ~1.1–3.7 kDa after calibration with PSS standards. The variations between different acids could be explained by their source and diagenetic stage, e.g. humic acids were generally larger than fulvic acids and *MM* and the polydispersity of acids from different sources increased in the order: surface water < soil < peat bog < lignite coal. Similar hydrodynamic sizes of humic substances have been determined by other techniques including fluorescence correlation spectroscopy, PFG-NMR, AFM [110] and SEC [111,126]. FlFFF has been used to study the variation in size of humic and fulvic acids with variations in pH [114] and ionic strength [114,117–119,126]. It was found that humic and fulvic acids could both decrease and increase in size when the pH was lowered [114], that an increase in ionic strength resulted in only a slight increase in polydispersity of fulvic acid, but a more pronounced increase in both size and polydispersity of humic acid [114,117–119,126], and that salts with divalent cat-ions (e.g. Ca^{2+}) had a more pronounced effect than monovalent (e.g. Na^{+}). These results were explained by protonation of the acids and screening of charges by counter-ions from the salts, resulting in contraction of the NPs due to lower intramolecular charge repulsion, and in aggregation of NPs, due to diminishing of the electrical double layers of the NPs. However, as stated in Section 7, size distributions determined by FlFFF under varying pH and ionic strength must be treated with caution, since the sample recovery of humic substances decrease rapidly with increasing cross-flow, decreasing pH and increasing ionic strength of the FlFFF-carrier, and is sensitive to the material of the accumulation wall membrane [33,113,114]. Variations in size could be a result of varying losses of smaller components by permeation through the accumulation wall membrane, or varying loss or retardation of hydrophobic components by membrane interactions.

8.2. River and lake waters

Typically 40–60% of the organic carbon, 50–100% of Fe and 30–70% of Al in natural freshwaters have been found to be associated with colloids (1–1000 nm particles) [127], of which a major portion is in the 1–100 nm size range, i.e. as NPs [67,77]. Association to NPs can largely influence the behaviour and transport of the trace elements and organic carbon in aquatic systems, and on-line coupling of FlFFF to ICP-MS has largely improved our understanding of these interactions [128]. For example, Hassellöv et al. showed that elements in a creek sample were distributed between two populations of NPs; 0.5–5 nm UV-absorbing organic colloids (presumed fulvic acid) and 5–25 nm iron rich NPs (presumed iron oxyhydroxide) [76]. Similar findings have been observed in the Amazon River and Rio Negro [120,129], the Kalix River in northern Sweden [69,70,130], the Loire River [43,72], peat-draining rivers in northern Scotland [131], and the lower Mississippi, Atchafalaya and Pearl Rivers in the southern USA [68] (Fig. 4a). The iron-rich NPs have also been identified by TEM–EDX in combination with FlFFF and ICP-MS [72]. Cu, Zn and U have shown to associate mainly to the UV-absorbing colloids, while Mn, Pb, P, Si and V associated strongly to the iron-rich NPs (Fig. 4b). These differences could often be explained by the chemistry of the elements [77,43,72] The sizes, concentrations and relative importance of the UV-absorbing and iron-rich NPs have been shown to vary between winter and spring flood in the Kalix River in northern Sweden [70,130] and with the hardness and the concentration and quality of organic matter in the Mississippi and Pearl Rivers in southern USA [65] (Fig. 4a). FlFFF has also shown that organic NPs are considerably larger in lake water than in river water, and varies in size between different rivers in the UK [42]. UV-absorbing NPs were larger in *MM* during high-slow periods than low-flow periods in rivers organic-rich rivers in Florida [86,121], and decreased in size from podsol soil solution to small creeks and large rivers in the Rio Negro basin [126]. The differences were explained by variations in diagenetic stage between rivers, lakes and podsol, and by variations in the erosion of organic NPs with varying flow.

The combined use of FlFFF, MALS, TEM and ICP-MS has shown the importance of considering particle shape when predicting element binding by river particles [43,72]. The FlFFF hydrodynamic radii of the particles has shown to match fairly well with the MALS gyration radii [43], while TEM particle radii in general has shown to be larger than FlFFF radii which can be attributed either to the deviations from spherical particle shape or the different size parameters measured by the different techniques (see Table 6).

AsFlFFF-ICP-MS has been used to determine the NP size distributions at different depths over the redox-cline in the Great Salt Lake, Utah, USA, showing the presence of several populations of NPs in the 1–12 nm size range with different binding of trace elements [132]. The results were taken as indications on the formation of metal–sulfide NPs at the oxic–anoxic interface.

8.3. Estuaries and marine water

FlFFF-ICP-MS has been used to study the changes in size of creek water colloids during mixing with synthetic seawater, and the results indicated aggregation of iron-rich NPs but lesser aggregation of UV-absorbing organic colloids [68]. The results have been confirmed in field studies in peat-draining rivers in northern Scotland, where iron-rich NPs decreased in concentration upon mixing

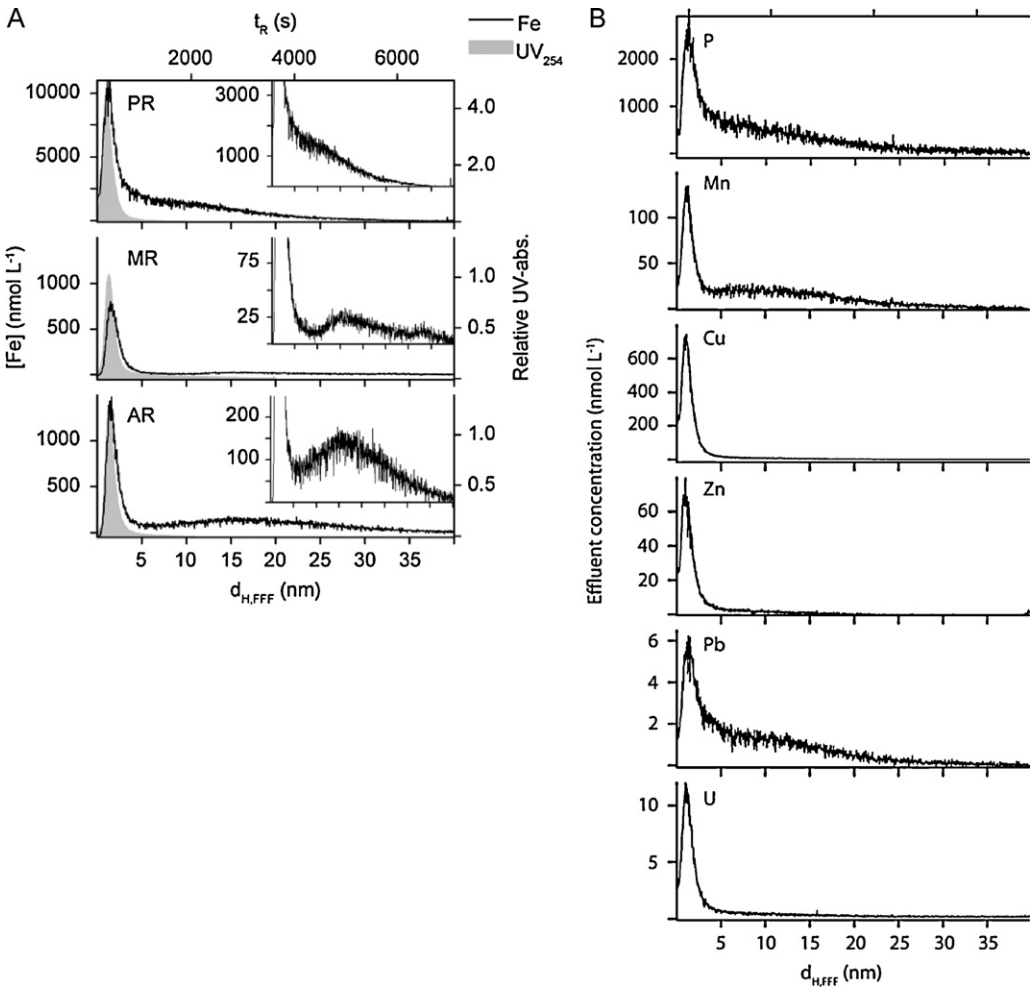

Fig. 4. (a) Size distributions of UV-absorbance and iron in the Pearl River (PR), lower Mississippi River (MR) and Atchafalaya River (AR) in the southern USA. The small inserted diagrams show the iron size distribution with the *y*-axis magnified. (b) Size distributions of different elements in the Pearl River. Figure modified from Stolpe et al. [65].

with seawater, while iron associated with organic matter showed a more conservative behaviour [131]. Moreover, in the brackish water of the Baltic sea, FlFFF-ICP-MS has shown that 0.5–4 nm UV-absorbing organic colloids are the dominant carriers for Fe, despite that the adjacent rivers carry large amounts of larger iron-rich NPs, suggesting estuarine removal of the iron rich NPs [133].

Even though the UV-absorbing organic macromolecules do not form large aggregates in contact with seawater, they have been shown to undergo smaller size transformations in the freshwater/seawater interface. For example, the MM and polydispersity of the UV-absorbing NPs in the Baltic sea, determined by FlFFF, were found to increase with increasing salinity, while humic-type fluorescent colloids increased in polydispersity but not in size [85]. In coastal waters in Florida, the MM of the UV-absorbing colloids decreased going from river to coastal seawater [125]. The variations were explained by removal of the larger and more reactive components of the colloids by photodegradation, biological activity and aggregation. In the Thurso Estuary, humic-like colloids mixed conservatively with seawater, but were observed to both decrease in size (observed from ultrafiltration and changes in optical properties) and increase in size (observed by dynamic light scattering and AsFlFFF) [75]. The results were explained by the contraction of individual macromolecules and aggregation between macromolecules due electrostatic screening. As stated previously, the results showing size transformation of UV-absorbing and iron-rich NPs with variations in salinity must be treated with some caution, since the recovery and membrane interactions of NPs in FlFFF can be expected to vary with ionic strength, with likely effects on the size distributions determined.

Studies of marine colloids using FlFFF have yielded contrasting results, probably due to differences in methodology (see Section 7), and due to the low concentrations and many different sources of colloids. UV-absorbing organic particles in coastal seawater from Maine showed one single population around 40–150 nm [124], while samples from the nearby Damariscotta River Estuary had a bimodal size distribution, with population at ~9 kDa, having a protein-like composition, and one population at ~75–250 kDa, having a humic like-composition (based on fluorescence) [74]. Similar size distributions were found in the off-shore waters of the Gulf of Mexico and in a planktonic cultures [74], while samples from the Mississippi River Plume had multiple populations in the 1–450 kDa size range, varying in concentration with depth, probably reflecting the input of organic matter from both plankton and sediment resuspension [74,135]. In a more recent study with FlFFF-ICP-MS, humic-like colloids in the Mississippi River Plume were found to be small (0.5–4 nm) and to bind most trace elements, while protein-like colloids were larger (3–7 nm) and were only binding P [65]. Similar results were found using AsFlFFF-ICP-MS, off-line coupled to AFM, to study samples from the Gullmarn Fjord in Sweden, where three populations of colloids were found; small (0.5–4 nm) humic-like rich organic matter from freshwater input, medium sized (3–7 nm) colloids (presumably protein-like) binding Ag, Cu

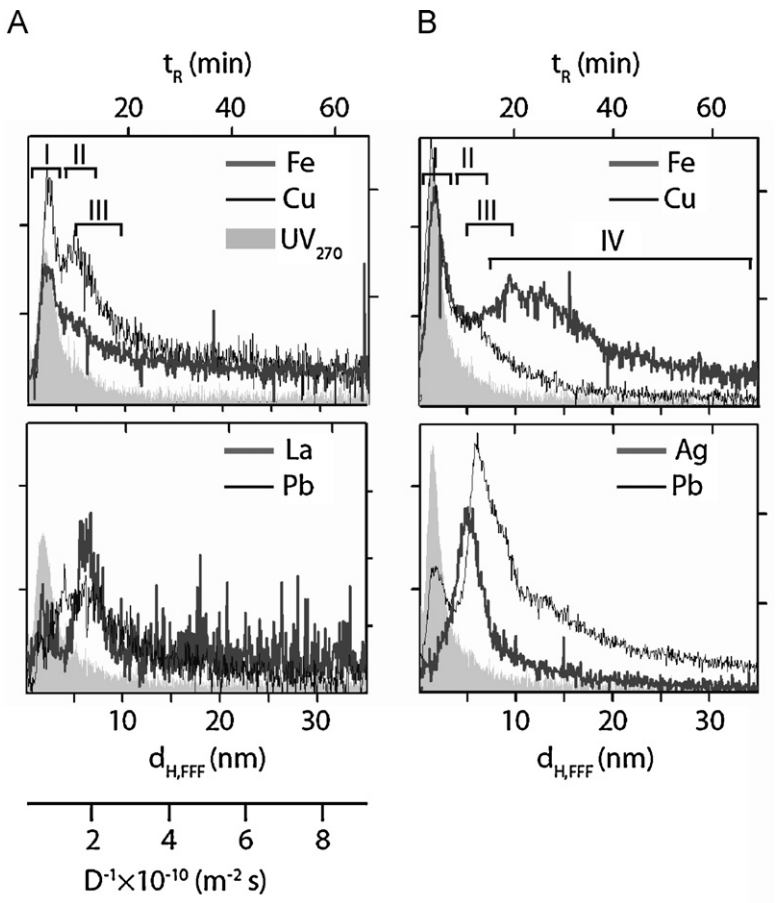

Fig. 5. Size distributions of UV-absorbance, Fe, Cu, Ag, La and Pb at 10 m depth in the Gullmarn Fjord on the Swedish west coast during maximum spring bloom (a), and after a long period of plankton blooms in June (b). Square brackets mark the size ranges of four hypothetical populations of NPs (I, II, III and IV), indicated by the size distributions of the different elements. Figure modified from Stolpe and Hassellöv [66].

and Pb, and 7–40 nm nanofibrils binding Fe and Pb (Fig. 5) [66]. It was hypothesized that the two larger populations of NPs were produced by marine organisms [65].

8.4. Wastewater

FlFFF has been little used for the characterization of the composition of wastewater samples and the few studies performed are summarized below. For instance, Amarasiriwardena and co-workers used FlFFF-ICP-MS for the size determination of organic colloids and associated trace elements in municipal wastewater [136]. Their analysis showed (i) a gradual reduction in concentration of organic colloids from primary through secondary treatment, (ii) the major fraction of Al, Cu, Fe, Pb, Mn and Zn was complexed to organic colloids and (iii) the precipitation and removal metal ions complexed to organic colloids as sludge. Prestel and co-workers used FlFFF-ICP-MS for the characterization of colloids in wastewater, showing similar results as the study by Amarasiriwardena and co-workers [137]. Additionally, their analysis showed a complete removal of >10 nm colloids, but only partial removal of fulvic/humic acids with a hydrodynamic diameter <10 nm. Klein and co-workers applied FlFFF to study the interaction of trace metals with colloids from a municipal waste disposal [138,139]. Their results showed that a substantial sorption of the heavy metals to colloids, in particular humic substances with hydrodynamic diameters of 1–10 nm. By AsFlFFF-ICP-MS, Worms et al. [140] found that Ag, Ce, Cu, Cr, Mn and Zn in wastewater treatment plant were associated with the low molar mass fraction (1.6–2.6 kDa) colloids, whereas Al, Fe and Pb were equally bound to low and high molar mass fractions. Beckett and co-workers applied FlFFF for the characterization of effluents from various streams within two pulp and paper mills situated in south-eastern Australia. FlFFF analyses showed that different effluent streams can have different *MM* distributions with effluents from the wood pulping process contained the highest *MM* components [141].

8.5. Soil, sediment and groundwater

Studies of the composition of soil particles using FlFFF have focused on different size fractions, by using different cross flow rates. Taken together, the results have shown the presence of small (a few nm) UV-absorbing organic colloids (presumed humic substances), medium sized NPs rich in Fe and Al (presumed iron oxyhydroxides), and large Al-rich particles (presumed clay particles) [142,143].

The occurrence of the iron rich NPs in soil, sediment and groundwater has been shown in several studies, but different conclusions have been drawn about their identities. Early studies using SdFFF-ICP-MS found that the Fe/Al ratio was higher below 150 nm than in larger size ranges [91,144,145], and explained the results by iron oxyhydroxide coating on clay particles. A later studies using FlFFF-ICP-MS to study particles in river sediment showed a similar shift in the size distributions of Fe and Al [57]. However, TEM–EDX measurements of the particles in the same study showed that the Fe occurred as discrete iron oxide NPs, while clay particles were much larger. Moreover, trace elements were associated with the iron oxide NPs to a much higher extent than to the clay particles, suggesting that the NPs are important for the transport of

trace metals in the sediment [57]. Contradictory to these results, FlFFF with a higher cross flow rate showed discrete 50–250 nm colloids in contaminated river sediment, but with higher Al than Fe-concentrations, indicating that clay particles were a more likely constituent than iron rich NPs [146]. In addition, in other studies, the iron rich NPs have been hypothesized to represent humic acid. For example, two populations of <10 nm NPs with different element-binding properties and pH-dependent solubility were found in wetland sediment extracts [147]. Similar results were found on small (<10 kDa) colloids from compost leachate [56,105] and organic-rich soil [148], where the size distributions of Al, Fe and Pb were centred at slightly larger *MM* (0.3 kDa difference) compared with the major population of UV-absorbing organic matter, Cr, Co, Ni and Cu. The authors have concluded that the two populations represented fulvic and humic acids, but in one of the studies, the larger NPs (presumed humic acids) decreased in concentration after the sample was treated with hydroxylamine, indicating iron oxyhydroxide as a major component [147].

There are strong indications on that iron rich NPs form during the oxidation of Fe(II) to Fe(III) in redox boundaries. In anoxic soil extract from organic-rich podsol, the size distributions of both UV-absorbance and humic substances were centred on one single population, a few nm in size [149]. However, when the extract was oxidized, the UV-absorbance showed a second 10–100 nm population, which gave no signal in humic-type fluorescence, indicating the formation of iron oxyhydroxide NPs. Similar results were found in anoxic river sediment, where a shift in the size distribution of Fe and other elements toward larger sizes indicated the formation of iron oxyhydroxide NPs [87].

The iron rich NPs have been found to bind trace elements and contaminants strongly, e.g. Cu, Pb [150], Th, lanthanides [151], As, Se, Sn and Pb [152,153]. For example, Eu-complexes with natural groundwater colloids showed higher stability than with isolated humic acid in contact with Chelex 100 (Bio-Rad) [154], and it was concluded that the high stability of the natural Eu-complexes was due to its incorporation in the matrix of inorganic NPs [154]. However, Bouby et al. showed that humic acid can make metal-clay particle complexes dissociate, by separating a suspension of clay particles spiked with Th and Eu, with and without humic acid present [155]. Eu, which form strong carbonate complexes, had a higher preference for the humic acid than Th, which mainly form hydroxy-complexes and therefore is more surface reactive.

Binding to iron rich and organic NPs can largely increase the mobility of trace elements in soil. For example there were strong evidence on that smaller (150 nm) Fe-rich particles were transported from the top soil to the sub-soil in a sandy soil profile, while larger (400 nm) particles with lower Fe/Al-ratios were trapped in the intermediate layers of the soil [156]. Moreover, the addition of synthetic iron oxide NPs largely increased the transport of Cu, Ni and Pb (by 30–70%) through a peat filter [157]. Reszat and Hendry studied the transport of different organic macromolecules between two chambers inserted in a natural till, and determined the diffusion coefficients of the compounds with AsFlFFF-UV [158]. Natural DOC (d = 1.7 nm, $D = 2.2 \times 10^{-10}$ m^2 s^{-1}) and small polystyrene sulfonate polymers (<1.75 nm) were able to diffuse through the till, isolated fulvic acid (d = 2.15 nm) diffused to a small extent while isolated humic acid (d = 2.7 nm, $D = 1.4 \times 10^{-10}$ m^2 s^{-1}) and larger (>3 kDa) polystyrene sulfonate polymers were not able to diffuse, due to straining in the pores of the till. In natural pore water samples, the overlap of the Zn and U size distributions with UV-absorbance showed that these elements bind to the fulvic acid [159], but it was estimated that this only comprise a small fraction of the total Zn and U in the pore water [159,160].

Very few studies have been conducted on NPs in groundwater from bedrock. Baik et al. used As-FlFFF coupled to LIBD and ICP-MS to characterize NPs in samples from boreholes in gneissic/plutonic bedrock in South Korea, and concluded that particles were a mixture of smaller (20–100 nm) calcite-rich NPs and larger (>100 nm) colloids rich in aluminosilicates and iron [161]. Cizdziel et al. studied NPs in seep water from a tunnel in the Yukka Mountains, USA, and found one population of small (a few nm) NPs, binding most elements, and a population of larger NPs, binding the halogens Cl, Br and I [162]. However, the authors concluded that the larger NPs could be calcite particles formed after sampling, due to increase in sample pH during storage.

8.6. Atmospheric particles

Airborne NPs constitute an important potential hazard to human health, due to their direct uptake by the lung [163] and consequent impacts on the cardio-vascular and other systems. Soot particles produced by diesel and gasoline engines have been characterized by both FlFFF and SdFFF [164–166]. Particles collected on filters placed on the exhaust line were extracted with ethanol and transferred to aqueous phase which were then analysed with FlFFF [165]. The size distributions determined by FlFFF and SdFFF differ somewhat, but there was a good agreement in the sizes determined by FlFFF, DLS, SEM and photon correlation spectroscopy (PCS). However, an on-line scanning mobility particle sizer (SMPS) gave a broader size distribution than the other techniques, suggesting dis-aggregation of particles during the sample preparation for the other techniques. Therefore, given the transfer to the aqueous phase required, the FlFFF data was more likely to represent the particle size distribution after wetting e.g. in lung fluid or surface waters. Particles were found to be distributed between 50 and 500 nm, often with a maximum around 100 nm in size [166]. Emission of particles was found to increase with load rate and speed of the engines, but the size distributions were not significantly different between heavy and light-duty diesel engines. Interestingly, the percentage of <100 nm particles were higher in the exhaust from a turbo-charged diesel engine than from a diesel engine with naturally aspirated inhalation system, and a catalytic converter on a gasoline engine narrowed the size distribution of particles from 50–600 nm to 50–250 nm [166].

9. Application for manufactured nanoparticles

The recent development of the field of nanotechnology, and in particular NPs (1–100 nm in size), enhanced the need for accurate particle separation and characterization. Particle size is one of the main parameters determining particle properties [8,167–174], and therefore is used in defining NPs in relation to their environmental behaviour and impacts [11,175,176]. The importance of size emphasises the need for an accurate and high-resolution method for NP size determination; it has been suggested in several publications and reports that FlFFF is a highly promising technique for the size separation and determination of NPs in complex media [177,178]. The applications of FlFFF in the area of manufactured NPs includes: NP size, composition, interaction with natural organic matter, measurement of the thickness of surface coating, structure (sphericity and permeability) and aggregation behaviour, and are discussed below and are summarized in Tables 4 and 5. Dieckman et al. [109] used FlFFF to determine the particle size distribution of L-cysteine-stabilized ZnS/Mn NPs, where they compared the FlFFF results to other size characterization methods such as TEM, analytical ultracentrifugation (AUC), dynamic light scattering (DLS) and X-ray diffraction (XRD). Converting all averages into mass weighted average size, they obtained comparable sizes with small differences following the order DLS > TEM > AUC > FlFFF ~ XRD. This is potentially due to the small size (<10 nm) and highly monodisperse nature of the NPs in these samples. The small differences obtained

Table 4
Summary of FlFFF operational conditions and analysis of manufactured nanoparticles.

Nanoparticle description	Device, detectors, membrane	Study objective	Injection volume	Pretreatment	Carrier solution	Operating conditions	Average size/size range (nm)	References
L-Cysteine-stabilized ZnS/Mn	AsFlFFF UV–VIS (280 nm) 5000 g/mol RC	Comparison of several techniques for measuring particle size distribution	NR	–	Water	CF 0.5 mL min^{-1} XF 2.0 mL min^{-1}	2.0–8.0	[109]
TiO_2, ZnO and quantum dots (QDs) at pH 4 and 8	FlFF (F-1000) UV (254 nm) 1 kDa RC	Comparison of FlFFF to other techniques including TEM, AFM, NTA, FCS and DLS	20 μL	–	10 mM $NaNO_3$	CF 1.0 mL min^{-1} XF 1.1 mL min^{-1} for QD XF 4.0 mL min^{-1}	TiO_2: weight average 3.7–8.2 Number average 1.3–2.1 QD: weight average 41.5 Number average 14.3	[17]
Cadmium selenide/zinc sulfide-mercaptoacetic acid core/shell-coated QD (CdSe/ZnS-MAA)	AsFlFFF UV (225 nm) ICP-MS 5 kDa RC	Characterization of particle size and composition	100 μL		Ultrapure water at pH 9.3	CF 0.8 mL min^{-1} XF decrease exponentially from 2.4 mL min^{-1} at the beginning to 0 after 30 min	Peak maximum 14.6 ± 0.5	[155]
SDS stabilized ZnO	FlFFF UV (254 nm) 10 kDa RC	Determining particle size distribution of ZnO NPs spiked in soil suspensions Studying the effect of aging on particle suspensions in soil	10–20 μL	Extracting the fraction <1 μm by gravitational sedimentation over night of the mixture of NPs and soil	0.2% (m/v) SDS in ultra-pure water	CF 1.0 mL min^{-1} XF 0.2 mL min^{-1}	ZnO NPs 50–450 ZnO NPs in soil 50–450	[179]
TiO_2	FlFFF (F-1000) UV (254 nm) ICP-AEM (off-line) 10 and 30 kDa RC	Characterize TiO_2 NPs extracted from commercial sunscreens products	20 μL	Particle extraction	Fl-70 anionic surfactant Triton X-100 nonionic surfactant	CF 2.040 ± 0.007 mL min^{-1} XF 2.968 ± 0.007 mL min^{-1}	50–350	[52]
Polyoxomolybdate NPs	FlFFF UV (455 nm) 10 kDa RC	Monitoring the growth of polyoxomolybdate NPs	NR	–	Triton X-100 nonionic surfactant	NR	3–75	[182]
Iron oxide NPs (hematite)	FlFFF UV (254) 1 kDa RC	Quantifying the thickness of the surface coating formed on iron NPs by Suwannee river humic acid (SRHA) Characterizing the aggregation of iron oxide NPs at a range of pH conditions (2–6)	20 μL	–	10 mM $NaNO_3$	CF 1.0 mL min^{-1} XF 0.5–1.1 mL min^{-1}	7 nm for single particles 50–500 nm for aggregates	[15]
Hematite NPs	FlFF (F-1000) FLD (Ex/Em: 380/250 nm) ICP-MS 1 kDa silicon coated RC	Analysis of pH dependent uranium (VI) sorption to hematite NPs	NR	–	0.01 vol% CTAB, 0.1 mM sodium azide, pH 5	CF 1.5 mL min^{-1} XF 0.5 mL min^{-1}	20–200	[181]
Citrate stabilized silver NPs	FlFFF 300 Da PES UV (400 nm)	Investigate the effect of OECD media for *Daphnia magna* toxicity tests on NP dispersion and aggregation	500 μL	–	10 mM NaCl	CF 1.0 mL min^{-1} XF 0.3–0.5 mL min^{-1}	7, 10, 20	[185]

Table 4 (*Continued*)

Nanoparticle description	Device, detectors, membrane	Study objective	Injection volume	Pretreatment	Carrier solution	Operating conditions	Average size/size range (nm)	References
Citrate, pectin and alginate stabilized silver NPs	FlFFF ETAAS UV (400 nm) 1 kDa RC acetate	Investigating the effect of NOM and ionic strength on the stability of AgNPs	20 μL	–	0.02% Fl-70 and 0.02% NaN_3 at pH 9.2–10	CF 1.0 mL min^{-1} XF 1.0 mL min^{-1}	9, 19 and 45 nm	[184]
Silver NPs	FlFFF UV (254 and 400 nm) ICP-MS DLS TEM 10 kDa RC	Investigates the use of FlFFF-ICP-MS as a sensitive and selective method for the detection and characterization of AgNPs. Characterization of AgNPs extracted from tissue of *Lumbriculus variegatus*		–	0.025% Fl-70 and 0.025% NaN_3 at pH 9.2–10	CF 1.0 mL min^{-1} XF 0.75 mL min^{-1}	10, 40 and 70 nm	[186]
Silver NPs	AsFlFFF UV (254 and 400 nm) ICP-MS	Investigating the effect of NOM and ionic strength on the stability of AgNPs	100 μL	–	5 mmol $NaNO_3$ at pH ~ 7.0	CF 0.3 mL min^{-1} XF 0.3–0.5 mL min^{-1}	10–500 nm	[183]
Polyphosphate stabilized Iron oxide NPs	AsFlFFF SAXS UV (400 nm) 10 kDa RC	Size separation and characterization of a given polydisperse sample of dispersed NPs	100 μL with an iron oxide concentration of 5.6 ± 0.3 mg/mL	–	0.1% (w/v) sodium polyphosphate	CF 0.3 mL min^{-1} XF 1.5–0.0 mL min^{-1}		[187]
C_{60} fullerene	AsFlFFF DLS TEM 10 kDa PES 10 kDa RC	Size fractionation of aqueous C_{60} fullerene aggregates in deionised water. Assessment of AsFlFFF-DLS on-line hyphenation	50–2000 μL	–	Deionised water	CF 1.0 mL min^{-1} XF 1.0–4.0 mL min^{-1}	80–260 nm	[40]

AEM: analytical electron microscopy; UF: ultrafiltration; CNT: carbon nanotubes; SWCNT: single-wall carbon nanotubes; MWCNT: multi-wall carbon nanotubes; PES: polyethersulfonate membrane; ETAAS: electrothermal atomic absorption spectroscopy.

Table 5
Summary of FlFFF calibration and data quantification methods and major conclusions of manufactured nanoparticle studies.

Nanoparticle description	Calibration calculation of R_h or M_w	Calculation/quantification	Main conclusions and comments	References
L-Cysteine-stabilized ZnS/Mn	–	–	FlFFF, AUC and DLS measure actual particle hydrodynamic diameter including a salvation or stabilizer shell, whereas TEM and XRD measures the diameter of the inorganic article core Underestimation of particle hydrodynamic diameter measured by AsFlFFF, possibly due strong charge interactions	[109]
TiO_2, ZnO and quantum dots	FlFFF theory and calibration with 20 nm spherical standards	Conversion of VPSD to NPSD and vice versa	Size measured by different techniques shows some discrepancies. This is related to the different parameters measured and the different weights of the measured distribution	[17]
Cadmium selenide/zinc sulfide-mercaptoacetic acid core/shell-coated QD (CdSe/ZnS-MAA)	Calibration with a series of spherical standards of different sizes (24, 105 and 207 nm)	DL for Zn and Cd are 28 and 11 μg/L	Constant Cd/Zn mass ratio suggesting a homogenous particle composition over the size range 10–30 nm. Increased Cd/Zn mass ratio after fractionation (0.53±) compared to (0.34) for the stock solution suggesting that part of Zn in the stock solution is present in a dissolved form	[155]
SDS stabilized ZnO	FlFFF theory	–	ZnO NPs are stable in the studied soil sample and stay mainly in liquid phase. They become partitioned between water and soil with aging, 7–14 days. FlFFF can be used to detect and characterize manufactured NPs in complex environmental matrix	[179]
TiO_2	FlFFF theory and calibration with a series of spherical standards of different sizes (46 ± 2.0 and 97 ± 3.0)	DL for Ti is 6–10 μg/L	Demonstrate the applicability of FlFFF-ICP-AES for the detection and size determination of TiO_2 NPs extracted from commercial sunscreens products	[52]
Polyoxomolybdate NPs	NR	NR	Polyoxomolybdate grow from small (3 nm), amorphous particles to larger NPs (25 nm) within 8 h and to macroscopic crystalline particles over several days	[182]
Iron oxide NPs	FlFFF theory and calibration with 20 nm spherical standards	–	Increase of surface film thickness with the increased concentration of SRHA up to 0.8 nm at 25 mg/L SRHA Aggregation of iron oxide NPs with the increase in pH in the range 2–6	[15]
Hematite NPs	NR	–	A comparison to sorption data analysed by centrifugation followed by filtration showed a good agreement with data collected by FlFFF. The uranium sorption to hematite increases as pH increase from 3 to 6.5	[181]
Citrate stabilized silver NPs	FlFFF theory and calibration with a series of spherical standards of different sizes (20 ± 2.0 and 30 ± 3.0)	–	Aggregation occurred heavily in the OECD test media. The aggregation was found to decrease with the dilution of the test media due to reduction in ionic strength. The 7 nm particles were found to be unstable under all media conditions	[185]
Citrate, pectin and alginate stabilized silver NPs	–	–	Citrate stabilized AgNPs are more borne to aggregation than pectin stabilized and alginate stabilized AgNPs as the later two types are sterically stabilized	[184]
Silver NPs	Calibration with a series of spherical standards of different sizes (20, 50 and 100 nm)	Recovery of silver as determined by ICP-MS 88–98%	AgNPs extracted from tissue of *Lumbriculus variegatus* increased in size from 31 to 46 nm indicating a change in NP characteristics during exposure	[186]
Silver NPs	Calibration with a series of spherical standards of different sizes (21 ± 1.5, 60 ± 2.5, 102 ± 3.0, 222 ± 6.0 and 486 ± 5 nm)	–	Aggregation of AgNPs occurred as ionic strength increased. This aggregation effect decreased in the presence of NOM	[183]
Polyphosphate stabilized iron oxide NPs	–	–	AsFlFFF-SAXS on-line coupling provides narrowly size-distributed fractions from a given nanoparticle sample	[187]
C_{60} fullerene	No calibration was used	Recovery of 77 ± 5.8%	This paper presents a methodology for aqueous C_{60} fullerene Size fractionation by AsFlFFF followed by size measurement by DLS (on-line) and mass determination by mass spectrometry (off-line)	[40]

here were attributed to the differences in measurement principles and measured parameters (see Table 6) [109]. Another comparative study of characterization of NPs (TiO_2 and quantum dots) by FlFFF compared to other techniques including TEM, atomic force microscopy (AFM), nanoparticle tracking analysis (NTA), fluorescence correlation spectroscopy (FCS) and DLS was performed by Domingos et al. [17]. Both of these studies suggest that there is no best technique for size determination of NP size, but a combination

Table 6
Comparison of FlFFF to the most commonly used sizing techniques for natural colloids and natural and manufactured nanoparticles.

Method	Measured parameter	Calculated size	Calculated average	References
FlFFF	Diffusion coefficient	Hydrodynamic diameter	Number average for FlFFF-LIBD Weight average for FlFFF-UV Mass average for FlFFF-ICP-MS Intensity average for FlFFF-MALLS	[45,96]
SEC	Particle size	Hydrodynamic diameter	Weight average	[105]
DLS	Diffusion coefficient	Equivalent hard sphere diameter	*Z*-average	[188]
TEM	2D projection	Minimum or maximum equivalent circular diameter	Number average	[189]
AFM	Height	Diameter	Number average	[101]
AUC	Sedimentation velocity	Hydrodynamic diameter	Mass weighted	[190]
UF filtration	Molar mass	–	–	[191]
XRD	Crystalline domain size	Crystalline domain size	Volume average	[192]
FCS	Diffusion coefficient	Equivalent hard sphere diameter	Intensity	[110]
LIBD	Particle size and concentration	Hydrodynamic diameter	Number	[96]
NTA	Diffusion coefficient	Hydrodynamic diameter	Number	[17]

SEC: size exclusion chromatography; DLS: dynamic light scattering; AUC: analytical ultracentrifugation; UF: ultrafiltration; XRD: X-ray diffraction; FCS: fluorescence correlation spectroscopy; NTA: nanoparticle tracking analysis.

of several techniques including FlFFF is the best approach to determine NP size [17,109], especially in complex matrices. However, in general this multi-method approach has not been used, given the time and resource requirements.

Isaacson and Bouchard have used FlFFF for the fractionation of aqueous C_{60} NPs followed by size determination by flow through and batch DLS and TEM [40]. The batch DLS was in good agreement with the flow through measurement, validating the use of DLS as an on-line detector with FlFFF. Additionally, sizes measured by TEM where in general agreement with the size determination by DLS.

Gimbert et al. (2007) have used FlFFF to detect, measure the size and monitor the partitioning of ZnO NPs spiked in soil suspension, demonstrating the applicability of FlFFF to determine the particle size distribution of manufactured NPs in complex environmental matrices [179]. They found that ZnO NPs rapidly equilibrate between soil and water and are relatively stable over 14 day period. Contado et al. applied the FlFFF-UV-ICP-MS to characterize TiO_2 NPs extracted from commercial sunscreens products [52].

Bouby et al. have used FlFFF-ICP-MS to determine the size distribution and chemical composition of CdSe/ZnS-MAA (mercaptoacetic acid) core/shell-coated quantum dots (QDs) [155]. The ratio of Cd/Zn of fractionated particles was determined and found to be higher than that for the unfractionated particles suggesting that part of the Zn in the unfractionated samples is present in a soluble form. FlFFF-ICP-MS was also used to quantify the sorption of uranium (VI) to haematite NPs [181]. A comparison to sorption data analysed by centrifugation followed by filtration showed a good agreement with data collected by FlFFF. Results show increased uranium sorption to hematite as solution pH increase from 3 to 6.5. This demonstrates the capacity of FlFFF-ICP-MS to study the speciation of trace metals, in particular for complex NP samples from natural waters (see Section 5).

The high resolution of FlFFF enabled the measurement of very small variations in particle size as a result of crystal growth and of surface film formation. For instance, Chen et al. (2005) used FlFFF together with other techniques such as UV, ICP-MS, SEM, TEM and AFM to monitor the growth of polyoxomolybdate NPs. They illustrated that polyoxomolybdate grow from small (3 nm), amorphous particles to larger NPs (25 nm) within 8 h and to macroscopic crystalline particles over several days [182]. Baalousha et al. have used FlFFF to quantify the thickness of the surface coating formed on iron oxide NPs by Suwannee river humic acid (SRHA). The surface coating thickness was observed to increase with the increase of the concentration of SRHA up to 0.8 nm at 25 mg/L SRHA [15]. In addition, the wide analytical window of FlFFF enabled haematite NP aggregation to be studied. Baalousha et al. studied the aggregation of iron oxide NPs at a range of pH conditions (2–6). Iron oxide NPs were found to be stable at low pH (2) and form larger aggregates of doublets at pH 3, triplets at pH 4 and larger aggregates at higher pHs [15].

Delay et al. have studied the affect of ionic strength and NOM on the stability of silver NPs and observed an increased destabilization effect with the increased ionic strength, whereas NOM was found to enhance the stability of the NPs due to the formation of a surface coating layer of NOM on the silver NPs [183]. The size and stability of citrate stabilized-, pectin stabilized- and alginate stabilized-silver NPs was investigated in the presence of NOM and in various types of environmental waters by FlFFF with off-line analysis by electrothermal atomic absorption spectrometry (ETAAS). Independent size measurements by DLS and TEM were in good agreement with values obtained by FlFFF. Citrate-stabilized silver NPs were more prone to aggregation compared to pectin stabilized- and alginate stabilized-silver NPs. Additionally, NOM was observed to prolongs the stability of silver NPs in the environment [184]. Römer et al. has used As FlFFF to study the aggregation and dispersion of silver NPs (AgNPs; 7, 10 and 20 nm) in OECD test media for *Daphnia magna* toxicity tests. They observed aggregation of the AgNPs in the OECD test media, which decreases with the dilution of the test media due to reduction in ionic strength. The smallest 7 nm NPs were found to be unstable under all media conditions [185]. Poda et al. has demonstrated the potential of FlFFF-ICP-MS for the detection and characterization of silver NPs extracted from tissue of the sediment dwelling, freshwater oligocharte *Lumbriculus variegates* at $\mu g\,L^{-1}$ concentration [186]. Particle size was found to increase from 31 to 46, suggesting an alteration of particle characteristics during exposure. Additionally, the measured sizes were found in good agreement with sizes measured by other sizing techniques such as DLS and TEM.

Knappe et al. have used FlFFF-small angle X-ray scattering (SAXS) for the preparation of monodisperse sample fractions originated from a highly polydisperse polyphosphate stabilized iron oxide NPs in aqueous suspension for use in toxicological studies. This study shows that FlFFF can also be used as a sample preparation tool to obtain monodisperse NPs of well-defined sizes ready to use to investigate their toxicological effects on cells [187].

The discussion presented here shows that FlFFF is finding more applications in the domain of NP characterization and more applications are expected in the near future. FlFFF is useful, not only for particle size determination, but also to gain more information on particle shape, optical properties, structure and composition.

10. Conclusions

Since the invention of FFF in 1966, there has been a slow growth in the application of this technique. This is mainly related to the difficulties with constructing the FFF system, the lack of commer-

cially available systems and the training required. The obstruction of commercially available systems was overcome in 1986 with the introduction of the first commercial FFF system, symmetric flow FFF; however, training remained an issue, in addition to sample preparation. In 1997, the first asymmetrical FFF system became available, where sample preparation became less of an issue, in particular for natural colloids and natural and manufactured NPs. Since then, FlFFF system has become more available for scientists and FlFFF is witnessing an increased application for the separation and characterization of natural and manufactured NPs in complex natural and biological media, and other particles and molecules that are beyond the remit of this review. The FlFFF has added an important dimension to the analytical toolkit available to environmental scientists and has added a wealth of information on natural colloids and increasingly on manufactured NPs. FlFFF, which is a major technique in the area of NP characterization. FlFFF allows continuous separation and sorting of complex samples as a function of diffusion coefficient/particle size, providing a continuous set (fractions) of monodisperse colloids/NPs, which simplifies further characterization of the particles. The high resolution, sensitivity, accuracy and possible hyphenation to a wide range of analytical techniques make FlFFF a powerful characterization tool. Elution profile can be used to monitor changes in size distributions of natural colloids and natural and manufactured NPs and therefore study processes such surface coating, aggregation and disaggregation. Eluents can be analysed by on-line detectors such as UV, OCD, FLD, MALS, LIBD, and ICP-MS, giving a wealth of information about particle size, shape and composition as well as associated trace pollutants. Fractions can be collected upon elution from FlFFF channel and analysed by TEM and AFM, giving more information about particle shape and chemical composition by ancillary TEM detectors such as X-EDS and EELS.

Acknowledgment

The authors would like to acknowledge funding from the UK Natural Environmental Research Council (the Facility for Environmental Nanoscience Analysis and Characterisation and NE/G004048/1).

References

[1] D.E. Giammar, C.J. Maus, L. Xie, Environ. Eng. Sci. 24 (2007) 85.
[2] D. Grasso, K. Subramaniam, M. Butkus, K. Strevett, J. Bergendahl, Rev. Environ. Sci. Biotechnol. 1 (2002) 17.
[3] T. Phenrat, H.J. Kim, F. Fagerlund, T. Illangasekare, R.D. Tilton, G.V. Lowry, Environ. Sci. Technol. 43 (2009) 5079.
[4] T.K. Darlington, A.M. Neigh, M.T. Spencer, O.T.N. Guyen, S.J. Oldenburg, Environ. Toxicol. Chem. 28 (2009) 1191.
[5] N.J. Rogers, N.M. Franklin, S.C. Apte, G.E. Batley, J.R. Lead, M. Baalousha, Environ. Chem. 7 (2010) 50.
[6] M.J.D. Clift, B. Rothen-Rutishauser, D.M. Brown, R. Duffin, K. Donaldson, L. Proudfoot, K. Guy, V. Stone, Toxicol. Appl. Pharmacol. 232 (2008) 418.
[7] K. Gao, X. Jiang, Int. J. Pharm. 310 (2006) 213.
[8] O. Choi, Z. Hu, Environ. Sci. Technol. 42 (2008) 4583.
[9] P. Christian, F. Von der Kammer, M. Baalousha, Th. Hofmann, Environ. Toxicol. Chem. 17 (2008) 326.
[10] J.R. Lead, K.J. Wilkinson, Environ. Chem. 3 (2006) 159.
[11] BSI, BSI British Standards, 2007.
[12] J.R. Lead, K.J. Wilkinson, in: J.R. Lead, K. Wilkinson (Eds.), Environmental Colloids: Behaviour, Structure and Characterisation, John Wiley and Sons, New York, 2007.
[13] N.S. Wigginton, K.L. Haus, M.F. Hochella, J. Environ. Monit. 9 (2007) 1306.
[14] M. Baalousha, J.R. Lead, F. Von der Kammer, Th. Hofmann, in: J.R. Lead, E. Smith (Eds.), Environmental and Human Health Effects of Nanoparticles, Wiley, Chichester, 2009, p. 109.
[15] M. Baalousha, A. Manciulea, S. Cumberland, K. Kendall, J.R. Lead, Environ. Toxicol. Chem. 27 (2008) 1875.
[16] M. Baalousha, Sci. Total Environ. 407 (2009) 2093.
[17] R.F. Domingos, M. Baalousha, Y. Ju-Nam, M. Reid, N. Tufenkji, J.R. Lead, G.G. Leppard, K.J. Wilkinson, Environ. Sci. Technol. 43 (2009) 7277.
[18] M.N. Myers, J. Microcol. Sep. 9 (1997) 151.
[19] W. Fraunhofer, G. Winter, Eur. J. Pharm. Biopharm. 58 (2004) 369.
[20] S. Levin, Biomed. Chromatogr. 5 (2005) 133.
[21] L.J. Gimbert, K.N. Andrew, P.M. Haygarth, P.J. Worsfold, TrAC Trend Anal. Chem. 22 (2003) 615.
[22] J. Liu, J.D. Andya, S.J. Shire, AAPS J. 8 (2006) E580–E589.
[23] F.A. Messaud, R.D. Sanderson, J.R. Runyon, T. Otte, H. Pasch, S.K.R. Williams, Prog. Polym. Sci. 34 (2009) 351.
[24] S.K. Ratanathanawongs, W.S. Lee, J. Sep. Sci. 29 (2006) 1732.
[25] T. Chianea, N.E. Assidjo, P.J.P. Cardot, Talanta 51 (2000) 835.
[26] L. Guglielmi, S. Battu, M. Le Bert, J.L. Faucher, P.J.P. Cardot, Y. Denizot, Anal. Chem. 76 (2004) 1580.
[27] M. Hassellöv, R. Kaegi, in: J.R. Lead, E. Smith (Eds.), Environmental and Human Health Effects of Nanoparticles, Wiley, Chichester, 2009, p. 211.
[28] R. Tatavarty, S. Shashadhar, L. Sungyun, K. Suhan, C. Jaeweon, I.S. Kim, J. Nanosci. Nanotechnol. 6 (2006) 2461.
[29] C. Giddings, Sep. Sci. 1 (1966) 123.
[30] C. Contado, A. Dalpiaz, E. Leo, M. Zborowski, P.S. Williams, J. Chromatogr. A 1157 (2007) 321.
[31] R. Beckett, B.T. Hart, in: J. Buffle, H. Van Leeuwen (Eds.), Environmental Particles, Lewis Publisher, Boca Raton, FL, USA, 1993, p. 165.
[32] M.H. Moon, D. Kang, J. Jung, J. Kim, J. Sep. Sci. 27 (2004) 717.
[33] B. Lyven, M. Hassellov, C. Haraldsson, D.R. Turner, Anal. Chim. Acta 357 (1997) 187.
[34] J.C. Giddings, Science 260 (1993) 1456.
[35] R. Beckett, Environ. Technol. Lett. 8 (1987) 339.
[36] S.A. Floge, M.L. Wells, Limnol. Oceanogr. 52 (2007) 32.
[37] S. Dubascoux, I. Le Hécho, M. Hassellöv, F. Von der Kammer, M. Potin Gautier, G. Lespes, J. Anal. At. Spectrom. 25 (2010) 613.
[38] M. Bouby, H. Geckeis, T.N. Manh, J.I. Yun, K. Dardenne, T. Schafer, C. Walther, J.I. Kim, J. Chromatogr. A 1040 (2004) 97.
[39] M. Baalousha, F.v.d. Kammer, M. Motelica-Heino, H. Hilal, P. Coustumer, J. Chromatogr. A 1104 (2006) 272.
[40] C.W. Isaacson, D. Bouchard, J. Chromatogr. A 1217 (2010) 1506.
[41] M. Baalousha, J.R. Lead, Environ. Sci. Technol. 41 (2007) 1111.
[42] M. Baalousha, J.R. Lead, Sci. Total Environ. 386 (2007) 93.
[43] M. Baalousha, F.v.d. Kammer, M. Motelica-Heino, P. Coustumer, J. Chromatogr. A 1093 (2005) 156.
[44] M. Baalousha, F.v.d. Kammer, M. Motelica-Heino, P. Coustumer, Anal. Bioanal. Chem. 308 (2005) 549.
[45] J.C. Giddings, in: M.E. Schimpf, K. Caldwell, J.C. Giddings (Eds.), Field Flow Fractionation Handbook, Wiley, New York, 2000, p. 3.
[46] M. Hassellöv, B. Lyvén, H. Bengtsson, R. Jansen, D.R. Turner, R. Beckett, Aquat. Geochem. 7 (2001) 155.
[47] K.D. Caldwell, in: M.E. Schimpf, K. Caldwell, J.C. Giddings (Eds.), Field Flow Fractionation Handbook, Wiley, New York, 2000, p. 79.
[48] T. Koch, J.C. Giddings, Anal. Chem. 58 (1986) 994.
[49] P.S. Williams, J.C. Giddings, Anal. Chem. 66 (1994) 4215.
[50] S. Assemi, G. Newcombe, C. Hepplewhite, R. Beckett, Water Res. 38 (2004) 1467.
[51] J. Calvin Giddings, P. Stephen Williams, M. Anna Benincasa, J. Chromatogr. 627 (1992) 23.
[52] C. Contado, A. Pagnoni, Anal. Chem. 80 (2008) 7594.
[53] R. Beckett, Z. Jue, C. Giddings, Environ. Sci. Technol. 21 (1987) 289.
[54] Y.P. Chin, P.M. Gschwend, Geochim. Cosmochem. Acta 55 (1991) 1309.
[55] P.J.M. Dycus, K.D. Healy, G.K. Stearman, M.J.M. Wells, Sep. Sci. Technol. 30 (1995) 1435.
[56] E. Bolea, F. Laborda, J.R. Castillo, Anal. Chem. Acta 661 (2010) 206.
[57] K.L. Plathe, F. Von der Kammer, M. Hassellöv, J. Moore, M. Murayama, T. Hofmann, M.F. Hochella, Environ. Chem. 7 (2010) 82.
[58] C. Deering, S. Tadjiki, S. Assemi, J. Miller, G. Yost, J. Veranth, Part. Fibre Toxicol. 5 (2008) 18.
[59] S. Tadjiki, S. Assemi, C.E. Deering, J.M. Veranth, J.D. Miller, J. Nanopart. Res. 11 (2008) 981.
[60] F.v.d. Kammer, S. Legros, T. Hofmann, E.H. Larsen, K. Loeschner, TrAC Trend Anal. Chem. 30 (2011) 425.
[61] R. Beckett, G. Nicholson, B.T. Hart, M. Hansen, J. Calvin Giddings, Water Res. 22 (1988) 1535.
[62] K.G. Wahlund, J.C. Giddings, Anal. Chem. 59 (1987) 1332.
[63] H. Lee, S.K.R. Williams, J.C. Giddings, Anal. Chem. 70 (1998) 2495.
[64] M. Hassellöv, B. Lyven, R. Beckett, Environ. Sci. Technol. 33 (1999) 4528.
[65] B. Stolpe, L. Guo, A.M. Shiller, M. Hassellöv, Mar. Chem. 118 (2010) 119.
[66] B. Stolpe, M. Hassellöv, Limnol. Oceanogr. 55 (2010) 187.
[67] B. Stolpe, M. Hassellov, K. Andersson, D.R. Turner, Anal. Chim. Acta 535 (2005) 109.
[68] B. Stolpe, M. Hassellov, Geochim. Cosmochim. Acta 71 (2007) 3292.
[69] R. Dahlqvist, M.F. Benedetti, K. Andersson, D. Turner, T. Larsson, B. Stolpe, J. Ingri, Geochim. Cosmochim. Acta 68 (2004) 4059.
[70] R. Dahlqvist, K. Andersson, J. Ingri, T. Larsson, B. Stolpe, D. Turner, Geochim. Cosmochim. Acta 71 (2007) 5339.
[71] S. Dubascoux, F. Von der Kammer, I. Le Hecho, M.P. Gautier, G. Lespes, J. Chromatogr. A 1206 (2008) 160.
[72] M. Baalousha, F. Kammer, M. Motelica-Heino, M. Baborowski, C. Hofmeister, P. Lecoustumer, Environ. Sci. Technol. 40 (2006) 2156.
[73] J. Boehme, M. Wells, Mar. Chem. 101 (2006) 95.
[74] M.L. Wells, Mar. Chem. 89 (2004) 89.
[75] S. Batchelli, F.L.L. Muller, M. Baalousha, J.R. Lead, Mar. Chem. 113 (2009) 227.
[76] Hassellöv, B. Lyven, C. Haraldsson, W. Sirinawin, Anal. Chem. 71 (1999) 3497.

[77] B. Lyven, M. Hassellov, D.R. Turner, C. Haraldsson, K. Andersson, Geochim. Cosmochim. Acta 67 (2003) 3791.
[78] R. Beckett, D. Murphy, S. Tadjiki, D.J. Chittleborough, C.J. Giddings, Colloids Surf. A: Physicochem. Eng. Aspects 120 (1997) 17.
[79] J.L. Weishaar, G.R. Aiken, B.A. Bergamaschi, M.S. Fram, R. Fujii, K. Mopper, Environ. Sci. Technol. 37 (2003) 4702.
[80] Y.P. Chin, G. Aiken, E. O'Loughlin, Environ. Sci. Technol. 28 (1994) 1853.
[81] E. O'Loughlin, Y.P. Chin, Water Res. 35 (2001) 333.
[82] Q. Zhou, S.E. Cabaniss, P.A. Maurice, Water Res. 34 (2000) 3505.
[83] S.A. Cumberland, J.R. Lead, J. Chromatogr. A 1216 (2009) 9099.
[84] T.N. Reszat, M.J. Hendry, Anal. Chem. 77 (2005) 4194.
[85] M. Hassellöv, Mar. Chem. 94 (2005) 111.
[86] E. Zanardi-Lamardo, C.D. Clark, C.A. Moore, R.G. Zika, Environ. Sci. Technol. 36 (2002) 2806.
[87] F.v.d. Kammer, M. Baborowski, S. Tadjiki, W.v. Tümpling, Acta Hydrochem. Hydrobiol. 31 (2003) 400.
[88] F.v.d. Kammer, M. Baborowski, K. Friese, J. Chromatogr. A 1100 (2005) 81.
[89] S.J. Hill, Inductively Coupled Plasma Spectrometry and Its Applications, Wiley-Blackwell, 2007.
[90] R. Beckett, Atom. Spectrosc. 12 (1991) 228.
[91] D.J. Chittleborough, D.M. Hotchin, R. Beckett, Soil Sci. 153 (1992) 341.
[92] H.E. Taylor, J.R. Garbarino, D.M. Murphy, R. Beckett, Anal. Chem. 64 (1992) 2036.
[93] D.M. Murphy, J.R. Garbarino, H.E. Taylor, B.T. Hart, R. Beckett, J. Chromatogr. 642 (1993) 459.
[94] T. Wagner, T. Bundschuh, R. Schick, R. Koster, Water Sci. Technol. 50 (2004) 27.
[95] C. Walther, S. Büchner, M. Filella, V. Chanudet, J. Colloid Interface Sci. 301 (2006) 532.
[96] M. Plaschke, T. Schafer, T. Bundschuh, T. Ngo Manh, R. Knopp, H. Geckeis, J.I. Kim, Anal. Chem. 73 (2001) 4338.
[97] R. Kaegi, T. Wagner, B. Hetzer, B. Sinnet, G. Tzvetkov, M. Boller, Water Res. 42 (2008) 2778.
[98] E. Alasonati, B. Stolpe, M.-A. Banincasa, M. Hassellov, V.I. Slaveykova, Environ. Chem. 3 (2007) 192.
[99] F.v.d. Kammer, PhD thesis pp 254, Hamburg University of Technology, 2005, p. 1.
[100] M.R. Schure, S.A. Palkar, Anal. Chem. 74 (2001) 684.
[101] K.J. Wilkinson, E. Balnois, G.G. Leppard, J. Buffle, Colloids Surf. A: Physicochem. Eng. Aspects 155 (1999) 287.
[102] R. Beckett, J. Ho, Y. Jiang, J.C. Giddings, Langmuir 7 (1991) 2040.
[103] Y.F. Dufrene, Proteomics 9 (2009) 5400.
[104] L.H. Hanus, H.J. Ploehn, Langmuir 15 (1999) 3091.
[105] E. Bolea, M.P. Gorriz, M. Bouby, F. Laborda, J.R. Castillo, H. Geckeis, J. Chromatogr. A 1129 (2006) 236.
[106] G. Newcombe, M. Drikas, S. Assemi, R. Beckett, Water Res. 31 (1997) 965.
[107] J. Cho, G. Amy, J. Pellegrino, Water Res. 33 (1999) 2517.
[108] D. Roessner, W.M. Kulicke, J. Chromatogr. A 687 (1994) 249.
[109] Y. Dieckmann, H. Colfen, H. Hofmann, A. Petri-Fink, Anal. Chem. 81 (2009) 3889.
[110] J.R. Lead, K.J. Wilkinson, E. Balnois, B.J. Cutak, C.K. Larive, S. Assemi, R. Beckett, Environ. Sci. Technol. 34 (2000) 3508.
[111] C. Pelekani, G. Newcombe, V.L. Snoeyink, C. Hepplewhite, S. Assemi, R. Beckett, Environ. Sci. Technol. 33 (1999) 2807.
[112] H. Thielking, W.M. Kulicke, J. Microcol. Sep. 10 (1998) 51.
[113] N.M. Thang, H. Geckeis, J.I. Kim, H.P. Beck, Colloids Surf. A: Physicochem. Eng. Aspects 181 (2001) 289.
[114] M.E. Schimpf, M.P. Petteys, Colloids Surf. A: Physicochem. Eng. Aspects 120 (1997) 87.
[115] J. Cho, G. Amy, J. Pellegrino, J. Membr. Sci. 164 (2000) 89.
[116] J. Cho, G. Amy, J. Pellegrino, Desalination 127 (2000) 283.
[117] M.-A. Benincasa, G. Cartoni, N. Imperia, J. Sep. Sci. 25 (2002) 405.
[118] G. Yohannes, S.K. Wiedmer, M. Jussila, M.L. Riekkola, Chromatographia 61 (2005) 359.
[119] A. Siripinyanond, S. Worapanyanond, J. Shiowatana, Environ. Sci. Technol. 39 (2005) 3295.
[120] M.F. Benedetti, J.F. Ranville, T. Allard, A.J. Bednar, N. Menguy, Colloids Surf. A: Physicochem. Eng. Aspects 217 (2003) 1.
[121] E. Zanardi-Lamardo, C.D. Clark, R.G. Zika, Anal. Chem. Acta 443 (2001) 171.
[122] M. Hassellov, B. Lyven, C. Haraldsson, W. Sirinawin, Anal. Chem. 71 (1999) 3497.
[123] S.K.R. Williams, R.G. Keil, J. Liq. Chromatogr. Relat. Technol. 20 (1997) 2815.
[124] R.D. Vaillancourt, W.M. Blach, Limnol. Oceanogr. 45 (2000) 485.
[125] E. Zanardi-Lamardo, C.A. Moore, R.G. Zika, Mar. Chem. 89 (2004) 37.
[126] E. Alasonati, V.I. Slaveykova, H. Gallard, J.P. Croue, M.F. Benedetti, Water Res. 44 (2010) 223.
[127] O.S. Pokrovsky, J. Schott, Chem. Geol. 190 (2002) 141.
[128] E.R. Sholkovitz, Geochim. Cosmochem. Acta 40 (1976) 831.
[129] J.P. Croue, M.F. Benedetti, D. Violleau, J.A. Leenheer, Environ. Sci. Technol. 37 (2003) 328.
[130] K. Andersson, R. Dahlqvist, D. Turner, B. Stolpe, T. Larsson, J. Ingri, P. Andersson, Geochim. Cosmochim. Acta 70 (2006) 3261.
[131] R. Krachler, R.F. Krachler, F. von der Kammer, A. Snphandag, F. Jirsa, S. Ayromlou, T. Hofmann, B.K. Keppler, Sci. Total Environ. 408 (2010) 2402.
[132] X. Diaz, W.P. Johnson, D. Fernandez, D.L. Naftz, Appl. Geochem. 24 (2009) 1653.
[133] J. Gelting, E. Breitbarth, B. Stolpe, M. Hassellov, J. Ingri, Biogeosciences 7 (2010) 2489.
[135] R.F. Chen, P. Bissett, P. Coble, R. Conmy, G.B. Gardner, M.A. Moran, X. Wang, M.L. Wells, P. Whelan, R.G. Zepp, Mar. Chem. 89 (2004) 257.
[136] D. Amarasiriwardena, A. Siripinyanond, R.M. Barnes, J. Anal. At. Spectrom. 16 (2001) 978.
[137] H. Prestel, L. Schott, R. Niessner, U. Panne, Water Res. 39 (2005) 3541.
[138] T. Klein, R. Niessner, Vom Wasser. Weinheim. 87 (1996) 373.
[139] T. Klein, R. Niessner, Mikrochim. Acta 129 (1998) 47.
[140] I.A.M. Worms, Z. Al-Gorani Szigeti, S. Dubascoux, G. Lespes, J. Traber, L. Sigg, V.I. Slaveykova, Water Res. 44 (2010) 340.
[141] R. Beckett, F.J. Wood, D.R. Dixon, Environ. Technol. 13 (1992) 1129.
[142] M. Hassellöv, F. Von der Kammer, Elements 4 (2008) 401.
[143] M.J. Hendry, J.R. Ranville, B.E.J. Boldt-Leppin, L.I. Wassenaar, Water Res. Res. 39 (2003) 1194.
[144] B. Chen, J. Hulston, R. Beckett, Sci. Total Environ. 263 (2000) 23.
[145] J.F. Ranville, D.J. Chittleborough, F. Shanks, R.J.S. Morrison, T. Harris, F. Doss, R. Beckett, Anal. Chim. Acta 381 (1999) 315.
[146] B.P. Jackson, J.F. Ranville, P.M. Bertsch, A.G. Sowder, Environ. Sci. Technol. 39 (2005) 2478.
[147] A. Siripinyanond, R.M. Barnesa, D. Amarasiriwardena, J. Anal. At. Spectrom. 17 (2002) 1055.
[148] C. Claveranne-Lamolère, G. Lespes, S. Dubascoux, J. Aupiais, F. Pointurier, M. Potin-Gautier, J. Chromatogr. A 1216 (2009) 9113.
[149] F. Kammer, U. Forstner, Water Sci. Technol. 37 (1998) 173.
[150] B. Chen, C.A. Shand, R. Beckett, J. Environ. Monit. 3 (2001) 7.
[151] H. Geckeis, T. Ngo Manh, M. Bouby, J.I. Kim, Colloid Surf. A: Physicochem. Eng. Aspects 217 (2003) 101.
[152] S. Dubascoux, I.Le Hθcho, M. Potin Gautier, G. Lespes, Talanta 77 (2008) 60.
[153] S. Dubascoux, J. Heroult, I. Le Hecho, M. Potin-Gautier, G. Lespes, Anal. Bioanal. Chem. 390 (2008) 1805.
[154] H. Geckeis, T. Rabung, T.N. Manh, J.I. Kim, H.P. Beck, Environ. Sci. Technol. 36 (2002) 2946.
[155] M. Bouby, H. Geckeis, F.W. Geyer, Anal. Bioanal. Chem. 392 (2008) 1447.
[156] J.F. Ranville, D.J. Chittleborough, R. Beckett, Soil Sci. Soc. Am. J. 69 (2005) 1173.
[157] Y. Kalmykova, S. Rauch, A.-M. Strömvall, G. Morrison, B. Stolpe, M. Hassellöv, Water Environ. Res. 82 (2010) 506.
[158] T.N. Reszat, M.J. Hendry, Environ. Sci. Technol. 43 (2009) 5640.
[159] T.N. Reszat, M.J. Hendry, Ground Water 45 (2007) 452.
[160] J.F. Ranville, M.J. Hendry, T.N. Reszat, Q. Xie, B.D. Honeyman, J. Contam. Hydrol. 91 (2007) 233.
[161] M.H. Baik, J.I. Yun, M. Bouby, P.S. Hahn, J.I. Kim, Korean J. Chem. Eng. 24 (2007) 723.
[162] J. Cizdziel, C. Guo, S. Steinberg, Z. Yu, K. Johannesson, Environ. Geochem. Health 30 (2008) 31.
[163] L.K. Limbach, Y. Li, R.N. Grass, T.J. Brunner, M.A. Hintermann, M. Muller, D. Gunther, W.J. Stark, Environ. Sci. Technol. 39 (2005) 9370.
[164] J.J. Kirkland, W. Liebald, K.K. Unger, J. Chromatogr. Sci. 28 (1990) 374.
[165] W.S. Kim, Y.H. Park, J.Y. Shin, D.W. Lee, S. Lee, Anal. Chem. 71 (1999) 3265.
[166] W.S. Kim, S.H. Kim, D.W. Lee, S. Lee, C.S. Lim, J.H. Ryu, Environ. Sci. Technol. 35 (2001) 1005.
[167] J.E. Spanier, R.D. Robinson, F. Zhang, S.-W. Chan, I.P. Herman, Phys. Rev. B 64 (2001), 245407–245407-8.
[168] I.V. Chernyshova, M.F. Hochella Jr., A.S. Madden, Phys. Chem. Chem. Phys. 9 (2007) 1736.
[169] P. Hoyer, H. Weller, Chem. Phys. Lett. 221 (1994) 379.
[170] Q. Chen, Z.H. Zhang, Appl. Phys. Lett. 73 (1998) 3156.
[171] D.M. Brown, M.R. Wilson, W. MacNee, V. Stone, K. Donaldson, Toxicol. Appl. Pharmacol. 175 (2001) 191.
[172] W.H. Qi, M.P. Wang, J. Nanopart. Res. 7 (2005) 51.
[173] A.S. Madden, J. Hochella, T.P. Luxton, Geochim. Cosmochim. Acta 70 (2006) 4095.
[174] V.H. Grassian, J. Phys. Chem. C 112 (2008) 18303.
[175] M. Baalousha, J.R. Lead, in: J.R. Lead, E. Smith (Eds.), Environmental and Human Health Effects of Nanoparticles, Wiley, Chichester, 2009, p. 1.
[176] Royal Society and Royal Academy, 2004.
[177] K. Tiede, A.B.A. Boxall, S.B. Tear, J. Lewis, H. David, M. Hassellv, Food Addit. Contam. 25 (2008) 795.
[178] M. Hassellöv, J.W. Readman, J.F. Ranville, K. Tiede, Ecotoxicology 17 (2008) 344.
[179] L.J. Gimbert, R.E. Hamon, P.S. Casey, P.J. Worsfold, Environ. Chem. 4 (2007) 8.
[181] E.K. Lesher, J.F. Ranville, B.D. Honeyman, Environ. Sci. Technol. 43 (2009) 5403.
[182] B. Chen, H. Jiang, Y. Zhu, A. Cammers, J.P. Selegue, J. Am. Chem. Soc. 127 (2005) 4166.
[183] M. Delay, T. Dolt, A. Woellhaf, R. Sembritzki, F.H. Frimmel, J. Chromatogr. A 1218 (2011) 4206.
[184] K. Songsilawat, J. Shiowatana, A. Siripinyanond, J. Chromatogr. A 1218 (2011) 4213.
[185] I. Römer, T.A. White, M. Baalousha, K. Chipman, M.R. Viant, J.R. Lead, J. Chromatogr. A 1218 (2011) 4226.
[186] A.R. Poda, A.J. Bednar, A.J. Kennedy, A. Harmon, M. Hull, D.M. Mitrano, J.F. Ranville, J. Steevens, J. Chromatogr. A 1218 (2011) 4219.

[187] P. Knappe, L. Boehmert, R. Bienert, S. Karmutzki, B. Niemann, A. Lampen, A.F. Thnnemann, J. Chromatogr. A 1218 (2011) 4160.
[188] F.L.L. Muller, Anal. Chim. Acta 331 (1996) 1.
[189] D. Mavrocordatos, D. Perret, G.G. Leppard, in: K.J. Wilkinson, J.R. Lead (Eds.), Environmental Colloids and Particles: Behaviour, Structure and Characterisation, John Wiley and Sons, Chichester, 2007.
[190] J.A. Jamison, K.M. Krueger, C.T. Yavuz, J.T. Mayo, D. LeCrone, J.J. Redden, V.L. Colvin, ACS Nano 2 (2008) 311.
[191] R. Liu, J.R. Lead, Anal. Chem. 78 (2006) 8105.
[192] T. Ungar, A. Borbqly, G.R. Goren-Muginstein, S. Berger, A.R. Rosen, Nanostruct. Mat. 11 (1999) 103.

Glossary

NPs: nanoparticles
FlFFF: flow field flow fractionation
AsFlFFF: asymmetrical flow field flow fractionation
SdFFF: sedimentation field flow fractionation
UV: ultraviolet
FLD: fluorescence detector
OCD: organic carbon detector
ICP-MS: inductively coupled plasma-mass spectroscopy
ICP-OES: inductively coupled plasma-optical emission spectrometry
LIBD: laser-induced breakdown detection
LS: light scattering
MALS: multi angle light scattering
AEM: analytical electron microscopy
TEM: transmission electron microscopy
SEM: scanning electron microscopy
STEM: scanning transmission electron microscopy
X-EDS: X-ray energy dispersive spectroscopy
AFM: atomic force microscopy
SEC: size exclusion chromatography
DLS: dynamic light scattering
UF: ultrafiltration
XRD: X-ray diffraction
AUC: analytical ultracentrifugation
FCS: fluorescence correlation spectroscopy
PFG-NMR: pulse field gradient-nuclear magnetic resonance
NTA: nanoparticle tracking analysis
RC: regenerated cellulose
CF: channel flow
XF: cross flow
FF: focus flow rate
DL: detection limit
PSS: polystyrene sulfonate
PES: polyether sulfone
SDS: sodium dodecyl sulfate
CNT: carbon nanotubes
SWCNT: single-wall carbon nanotubes
MWCNT: multi-wall carbon nanotubes
DOC: dissolved organic carbon
kDa: kilo Dalton
R_h: hydrodynamic diameter
R_g: radius of gyration
MM: molar mass
VPSD: volume particle size distribution
NPSD: number particle size distribution